CHAPTER - 3

STUDIES OF WATER-SOLUBLE POLYMERS

3.1 Preview

3.2 Results and Discussion

- i) Infrared Spectroscopy
- ii) Nuclear Magnetic Resonance
- iii) Reactivity Ratios
- iv) Thermogravimetric Analysis
- v) Differential Scanning Calorimetry
- vi) Viscosity Studies

3.1 Preview

Research on polymers has been addressed to 'tailor made' polymers with specific physical and chemical properties. For studying the potential of new polymer systems for commercial applications, it is desirable to characterize them for chemical composition, tacticity, sequence distribution of the monomer units in the polymer chains and correlate them with the physical and chemical properties of these copolymers. Spectroscopic characterization methods are also important aspects for getting information about the chemical structure of the polymers.

The spectroscopic methods involved are infrared (IR) spectroscopy and nuclear magnetic resonance spectroscopy. The success of IR spectroscopy in the characterization of organic compounds is a result of the almost general validity and applicability of the concept of group frequencies[275]. The importance of IR spectroscopy is considerably enhanced by its ability to provide detailed information on the microstructure of polymers. This includes the way in which the successive monomer units add on the existing chain, both in case of homo and copolymers, the configurational and conformational structure of the chains, and the chain end groups.

The use of nuclear magnetic resonance (NMR) spectroscopy for the microstructural analysis of polymers has grown spectacularly during the past decade or so. The stimulus for this growth was the demonstration in the early 1960's that high resolution ^{1}H-NMR could be used to determine the tacticity of some acrylic acid and vinyl homopolymers, and to assess the distribution of monomer units in some simple addition copolymers[276]. ^{13}C-NMR spectroscopy offers several advantages over ^{1}H-NMR for polymer chemists. The much larger range of chemical shifts observed for carbon nuclei in polymer chains compared to those of protons, enables the microstructural differences to be detected more readily by ^{13}C-NMR than by ^{1}H-NMR. The main information that can be obtained from ^{13}C-spectra are : identification of specific polymers, branching in macromolecules, analysis of sequences in

copolymers, distinction between block and random copolymers and analysis of microtacticity[277].

Knowledge of the sequence distribution of the monomers in the polymer chains may supply information about the process of addition of monomers during radical copolymerization. Such structural findings have become possible with the advent of ^{13}C-NMR spectroscopy. The elemental analysis data also gives knowledge of the structural compositions of the monomers incorporated within the copolymers[278]. In order to get maximum useful information, non-spectroscopic studies of polymer should be combined with polymer spectroscopy. This gives a better understanding of the polymer samples being studied.

Thermo analytical techniques are being extensively used to characterize a polymer to measure the temperature dependence of some of the mechanical or physical property and to correlate it to the structure[279]. They involve a group of techniques in which properties are measured as a function of time or temperature, keeping every other variable constant[280,281].

Thermogravimetric analysis (TGA) involves continuous monitoring of the weight of the sample with temperature, at a constant rate of change of time (isothermally) or of temperature. The most common usage of TGA is in measuring the thermal and oxidative stability of polymers under working conditions. The sample evolves a volatile product from the parent compound, then useful information is obtained from this technique[282,283].

Differential scanning calorimetry (DSC) is another method to monitor the effect of heat changes on a polymer sample. In a DSC unit the record of heat flow is done directly as a function of temperature. The sample and the reference material both are maintained at an isothermal condition in DSC by the required flow of electrical energy as they are heated or cooled. The area enclosed by a DSC curve is proportional to the enthalpy change[284]. The proportionality constant is independent of temperature in DSC.

Among the solution properties, the most useful and common method for polymer characterization is viscosity. The solution viscosity is helpful to determine polymer molecular weight and it has been so recognized since the early work of Staudinger[285]. Solution viscosity is basically a measure of the size or extension in space of polymer molecules. The simplicity of measurement and usefulness of viscosity-molecular weight correlation is so much that the viscosity - measurement constitutes an extremely valuable tool for molecular characterization of polymers[286,287]. The viscosity characteristics of polyacrylamide solutions show unique dependence on time[288]. The copolymers of acrylamide and acrylic acid are affected by nature of salts and of pH. Many studies have been carried out on the complexities of the solution behaviour of polyacrylamide and its copolymers[289,290].

In the present work, the above mentioned methods were used for characterization.

3.2 Results and Discussion

i) Infrared Spectroscopy

The homopolymers PAA and PAAc showed characteristics IR absorptions which agreed very well with those reported in literature[291,292]. The IR spectrum of PAA (Fig. 10) showed strong absorption at 1650 cm^{-1} due to the C=O bond of the carbonamide group. The medium absorption at 1400 cm^{-1} was due to C-N stretch. The IR spectrum of PAAc (Fig.14) shows a broad absorption band due to the O-H band present in the -COOH group in the range of 3300-3500 cm^{-1} [293]. The C=O bond of carboxylic acid was observed at 1720 cm^{-1}. Two bands arising from C-O stretching and O-H bending appear in the spectrum. These are ~ 1320-1210 cm^{-1} and 1440-1395 cm^{-1} respectively. Both of these bands involve some interaction between C-O stretching and in plane C-O-H bending[294].

The IR spectra of the copolymers P(AA-AAc) show absorption bands typical of constituent monomeric units and their relative intensities, depending on composition.

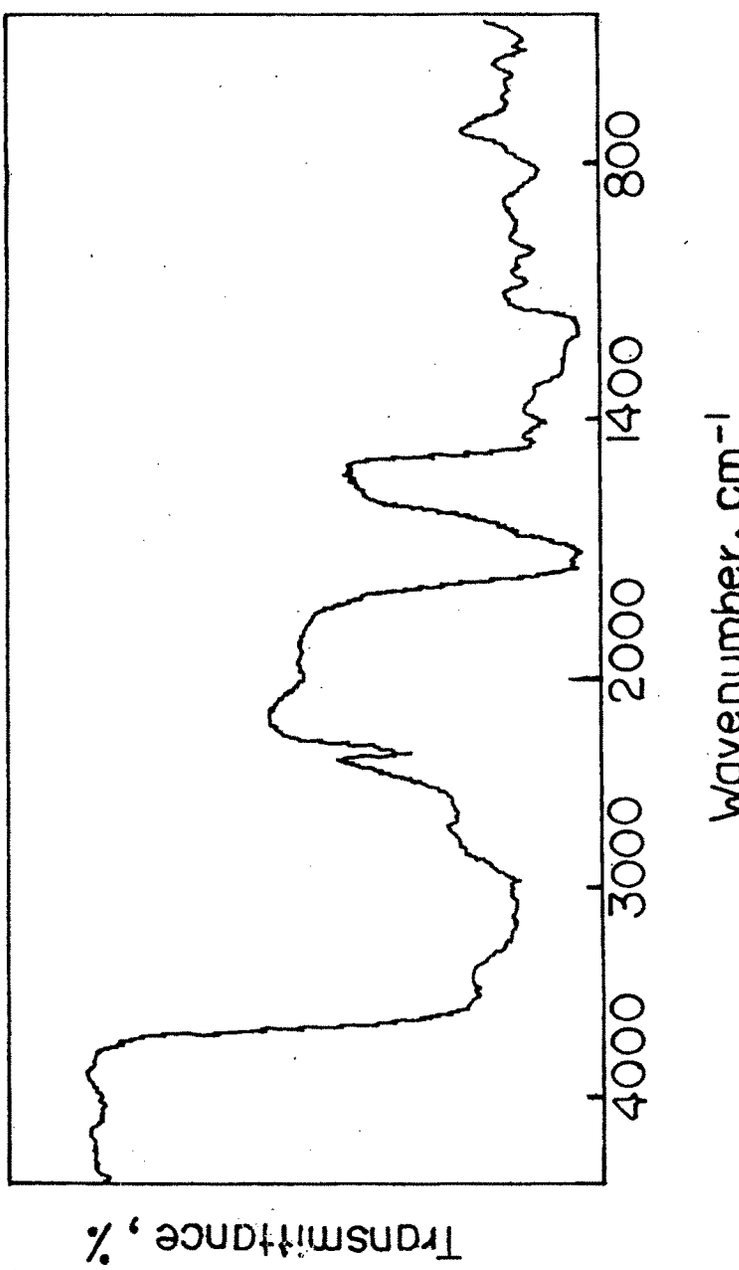

Fig. 10.: IR spectrum of polyacrylamide.

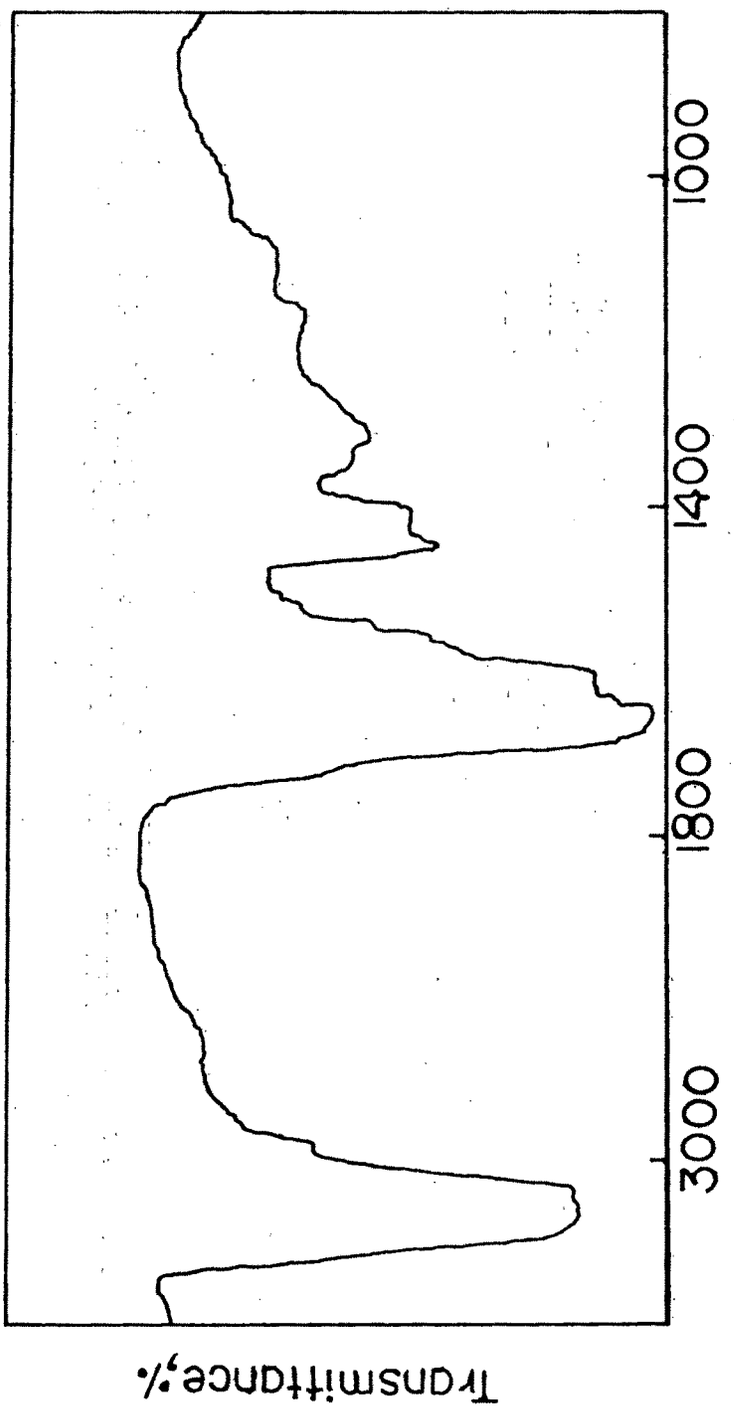

Fig. 11 : IR spectrum of P(AA-AAc) 85:15 copolymer.

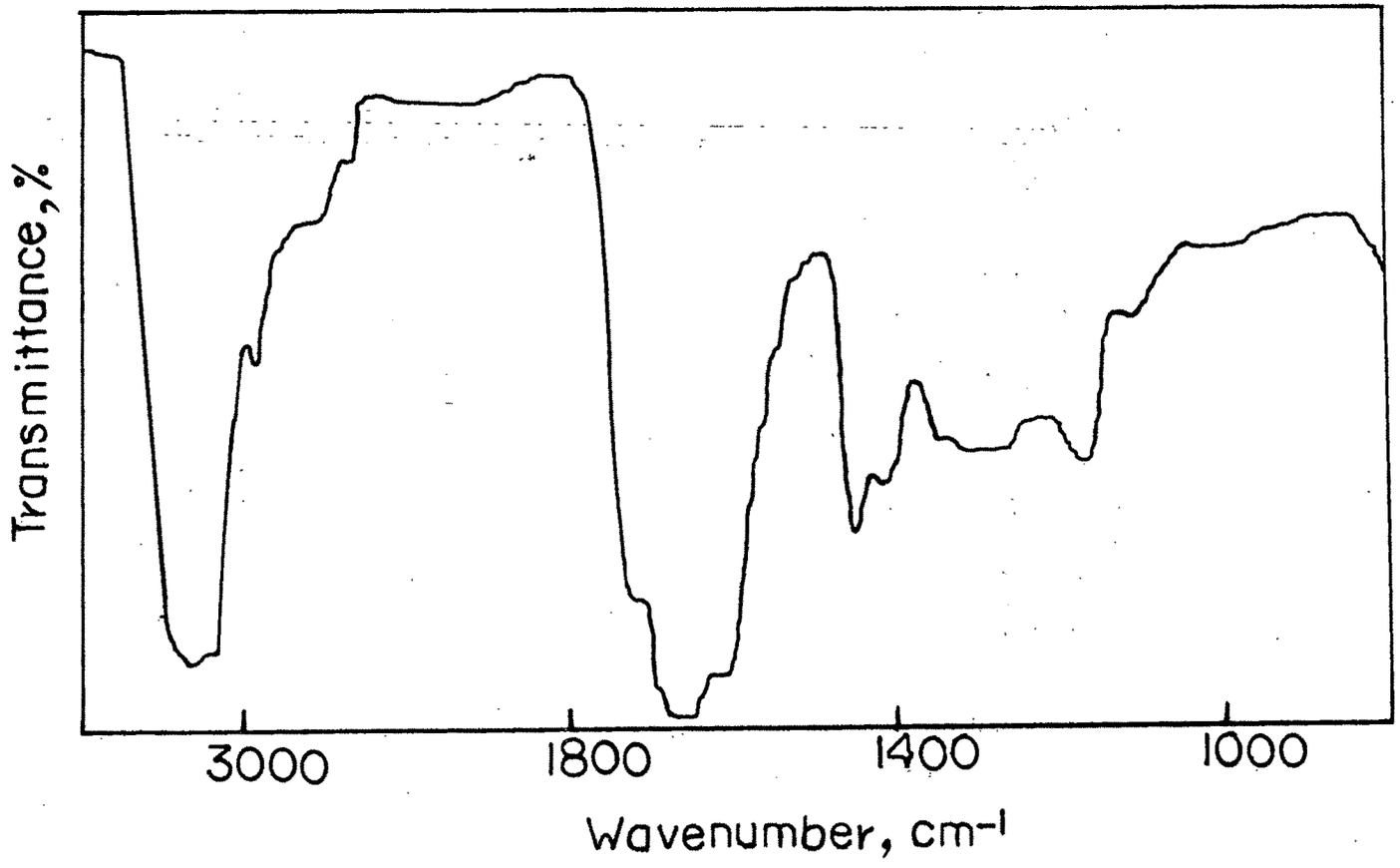

Fig. 12 : IR spectrum of P(AA-AAc) 65:35 copolymer.

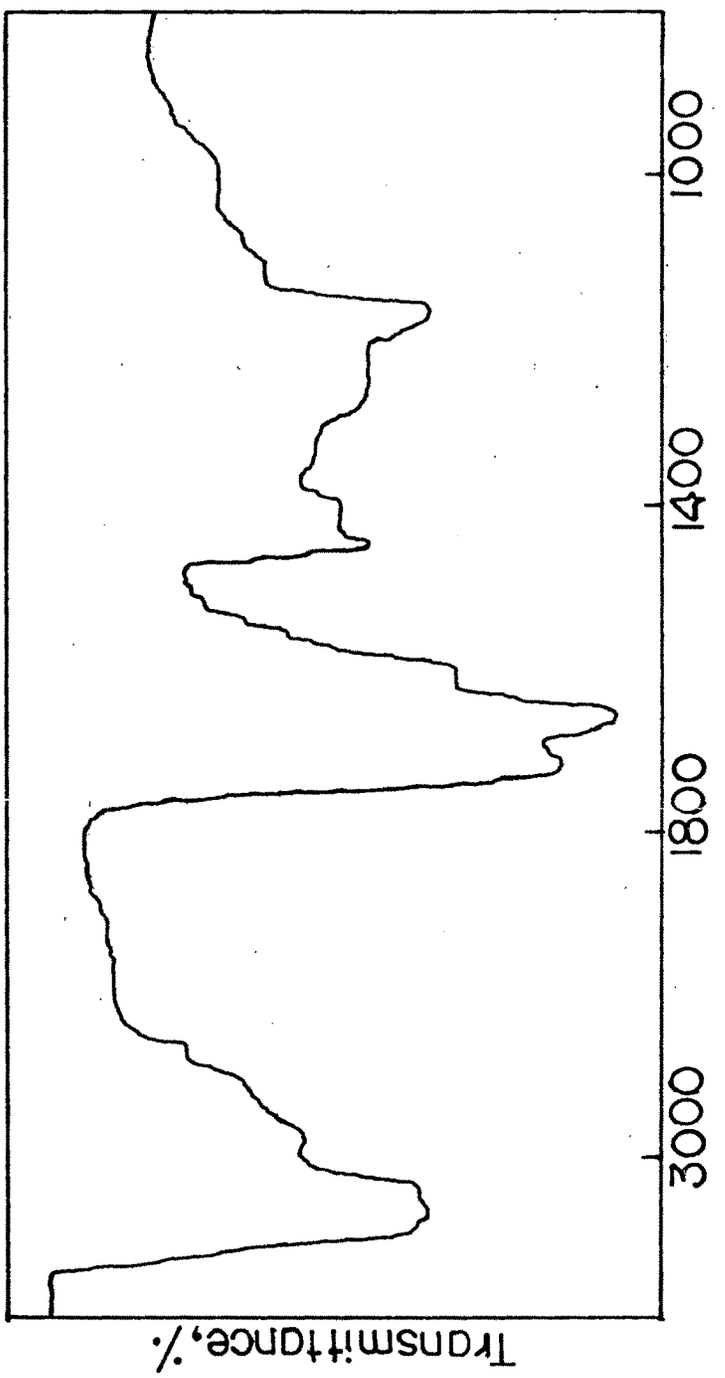

Fig. 13 : IR spectrum of P(AA-AAc) 50:50 copolymer.

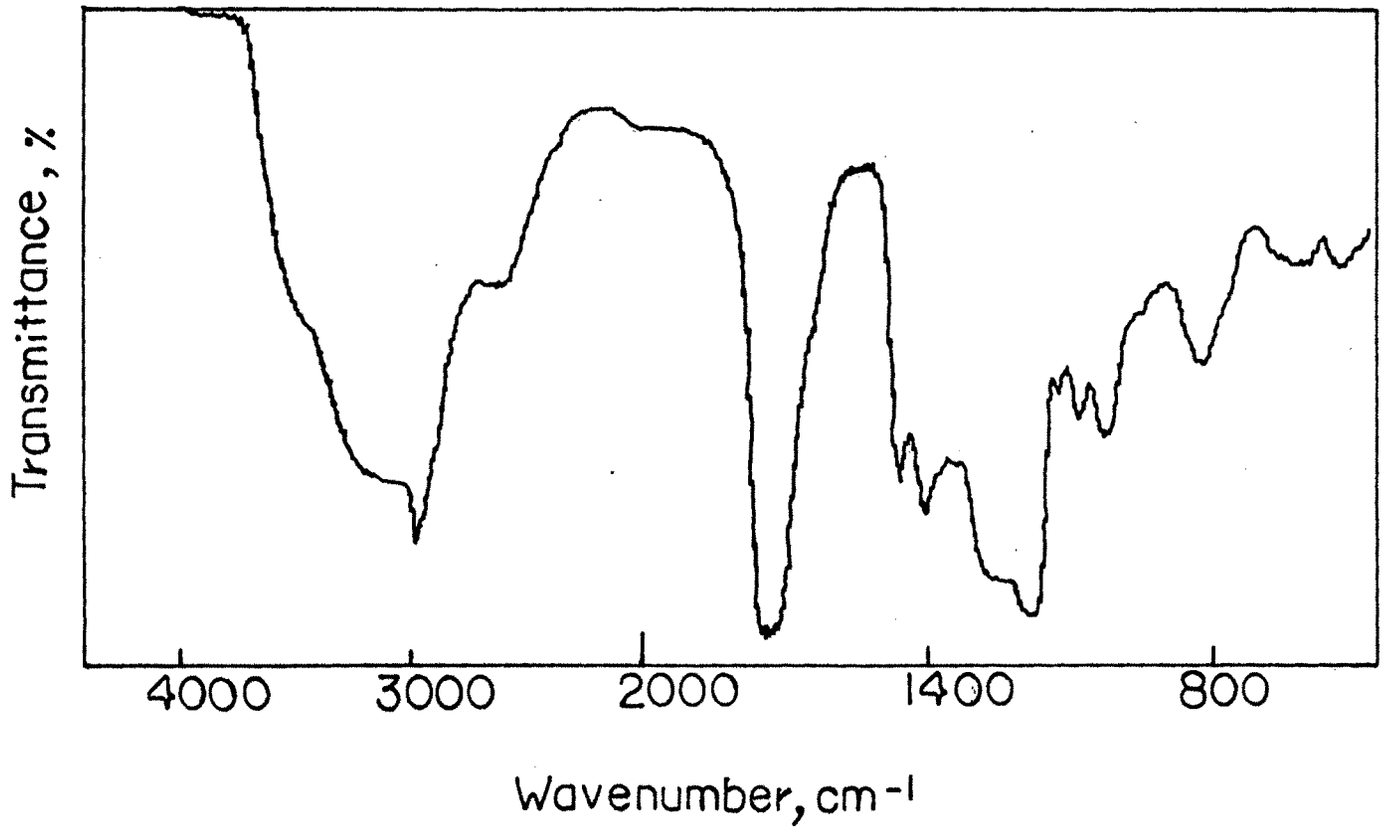

Fig. 14 : IR spectrum of polyacrylic acid.

The IR spectra of the copolymers is given in Figs.11-13. In the IR spectra of the 65:35 ratio of the copolymer, the C=O bond of the carbonamide group absorbs at 1650 cm^{-1}. The C-N stretching bond of primary amide was absorbed near 1400 cm^{-1} [291]. In the 50:50 ratio of copolymer the broad absorption band at 3300 cm^{-1} is absorbed due to O-H bond of the COOH group and also the C-N stretching band at 1400 cm^{-1}.

ii) Nuclear Magnetic Resonance Spectroscopy :

Further evidence of the two monomers being incorporated is given by NMR-spectroscopy. In the ^{1}H-NMR spectra of PAA (Fig. 15) the methylene (-CH_2) protons appear as a broad peak at δ = 1.6-1.8 ppm[295]. The methine protons resonate at δ = 2.28 ppm. On incorporation of AAc moiety the extra peak is observed at δ = 2.84 ppm due to the backbone methine proton (-CH) adjacent to carboxylic acid. With increase in acrylic acid moiety in the copolymers, the intensity of peak increases (Figs. 16,17).

The ^{13}C-NMR spectra of the polymers also show the corresponding groups being present. The ^{13}C-NMR spectra of PAA is given in Fig.18. The chemical shift values of PAA are in agreement with those reported earlier[292,296,297]. The methine carbon (-CHCONH$_2$-) of the backbone resonates at 44.744 ppm and the backbone methylene carbon resonates between 36.768-38.971 ppm. The carbonyl carbon appeared as a sharp singlet at 182.365 ppm. In case of copolymers an extra peak due to methine carbon (-CHCOOH) was observed at δ= 63.97 ppm[295,298]. The intensity of this peak increased with the increase in the incorporation of AAc. The carbonyl carbon of the -COOH group absorbs at δ=178.399 - 179.345 ppm. The intensity of this peak also increased with the increase in AAc content (Figs.19,20). The absorptions of the backbone -CH_2 from both the monomers could not be distinguished from ^{13}C-NMR spectra. The ^{13}C-NMR spectra and proton spectra are complimentary to each other.

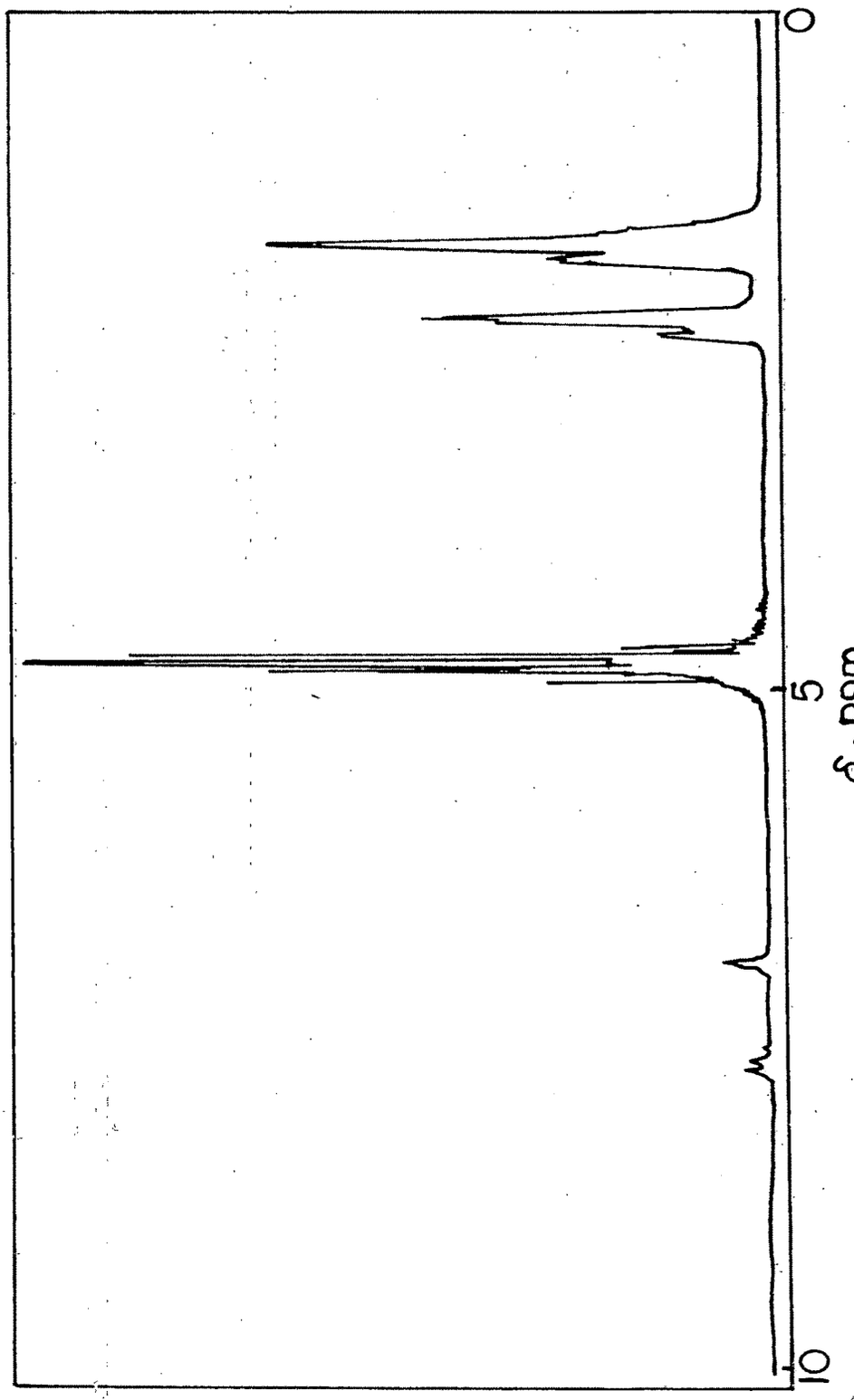

Fig. 15 : Proton NMR spectra of polyacrylamide.

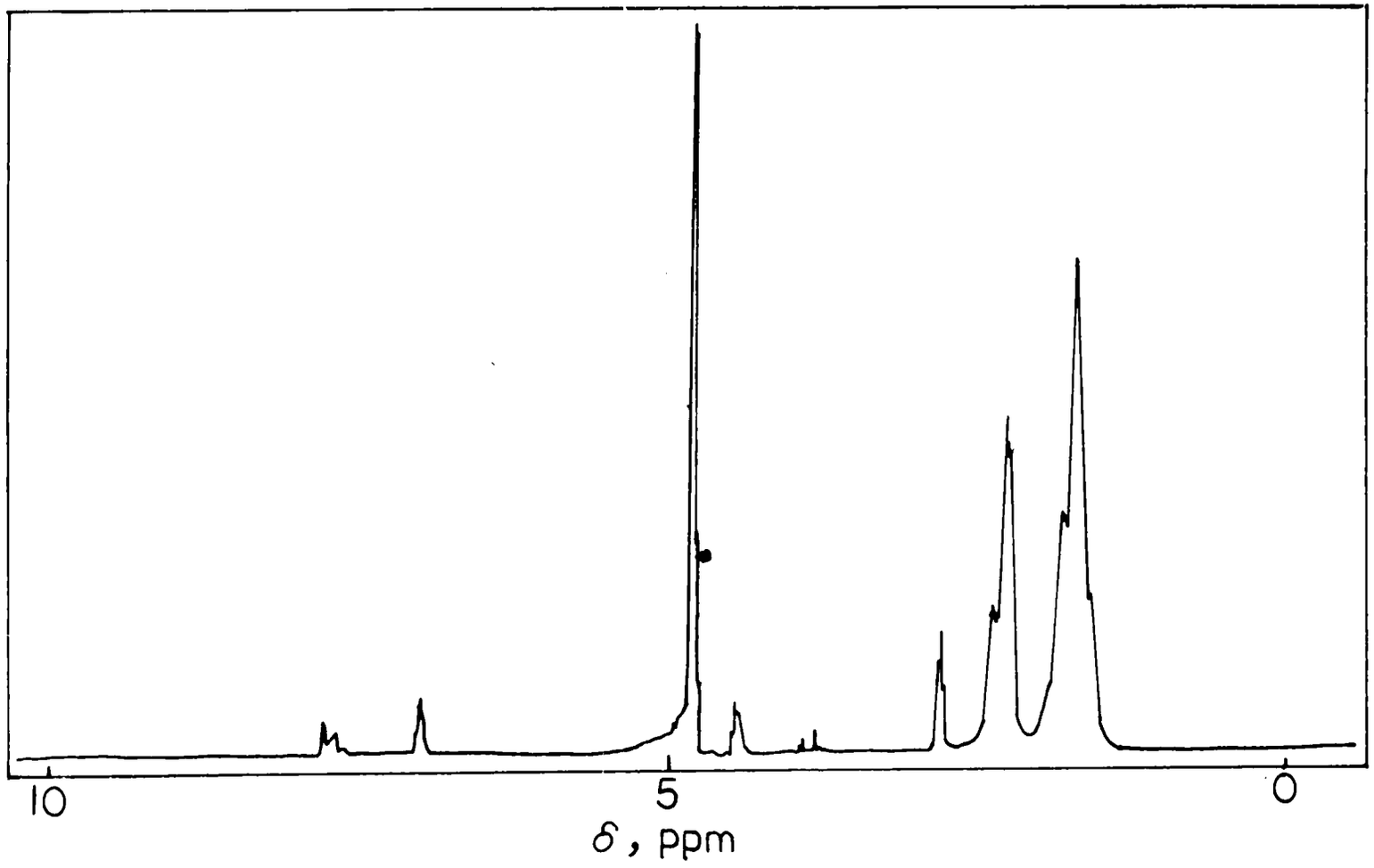

Fig. 16 : Proton NMR spectra of P(AA-AAc) 85:15 copolymer.

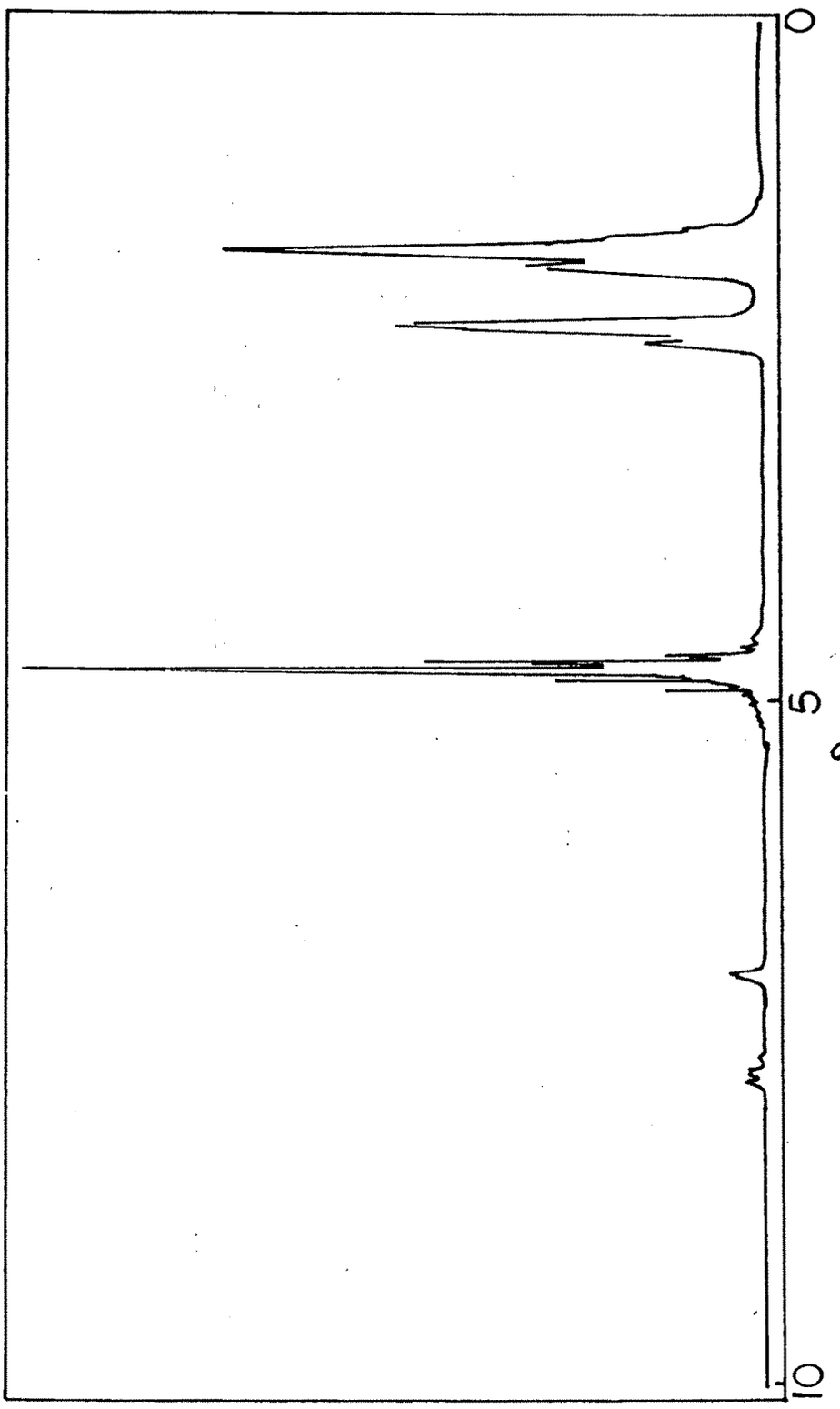

Fig. 17 : Proton NMR spectra of P(AA-AAc) 65:35 copolymer.

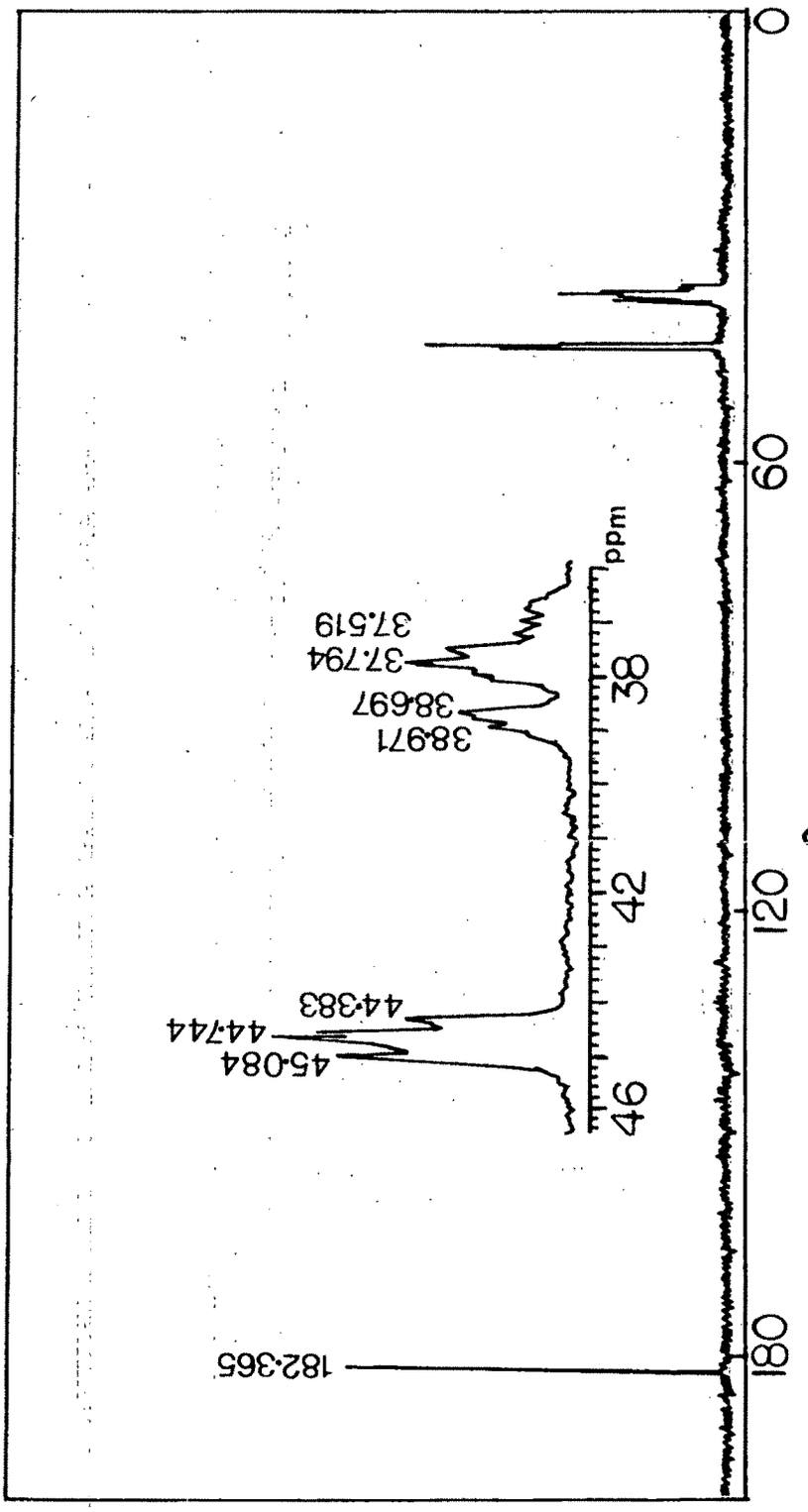

Fig. 18 : ^{13}C-NMR spectra of polyacrylamide.

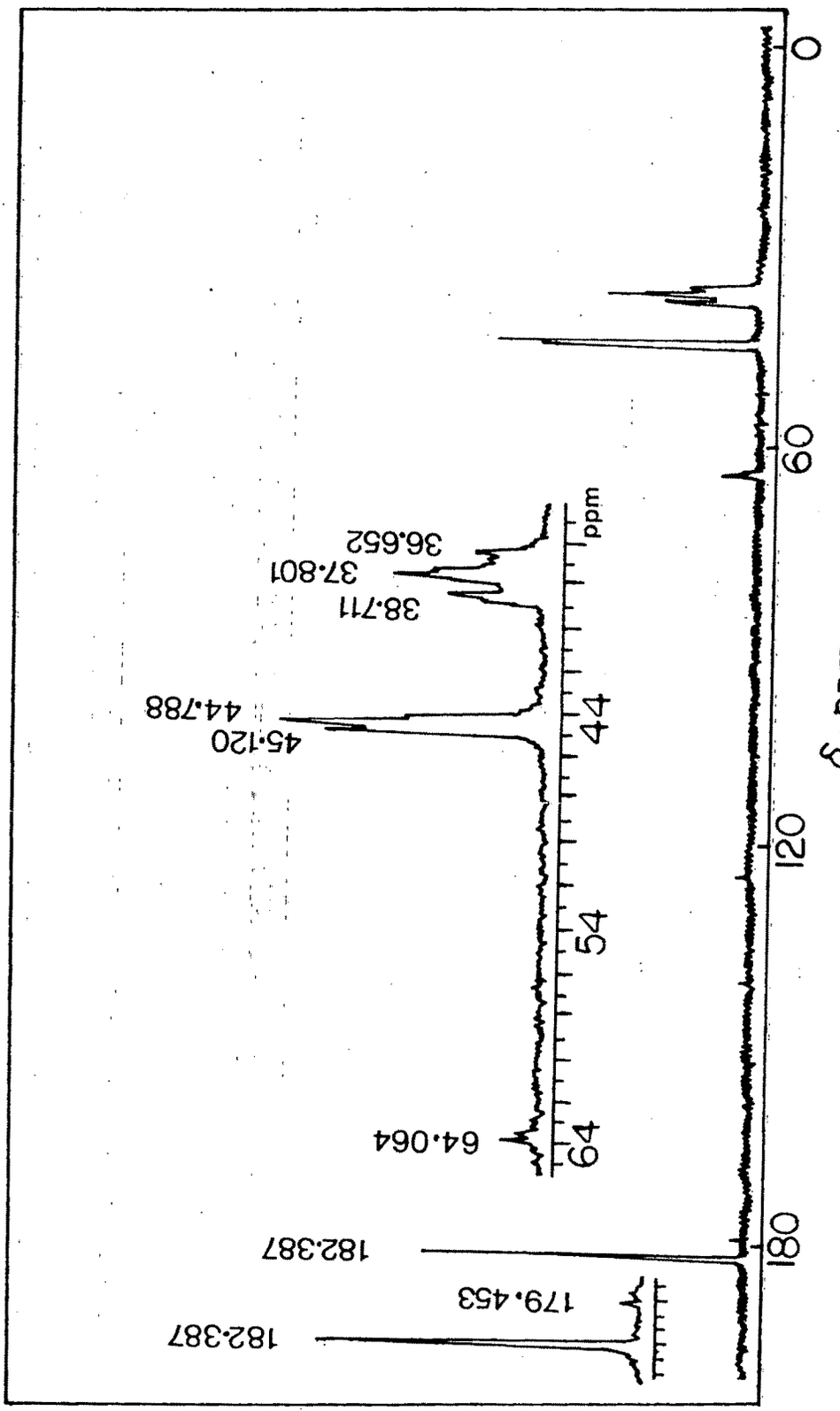

Fig. 19 : ^{13}C-NMR spectra of P(AA-AAc) 85:15 copolymer.

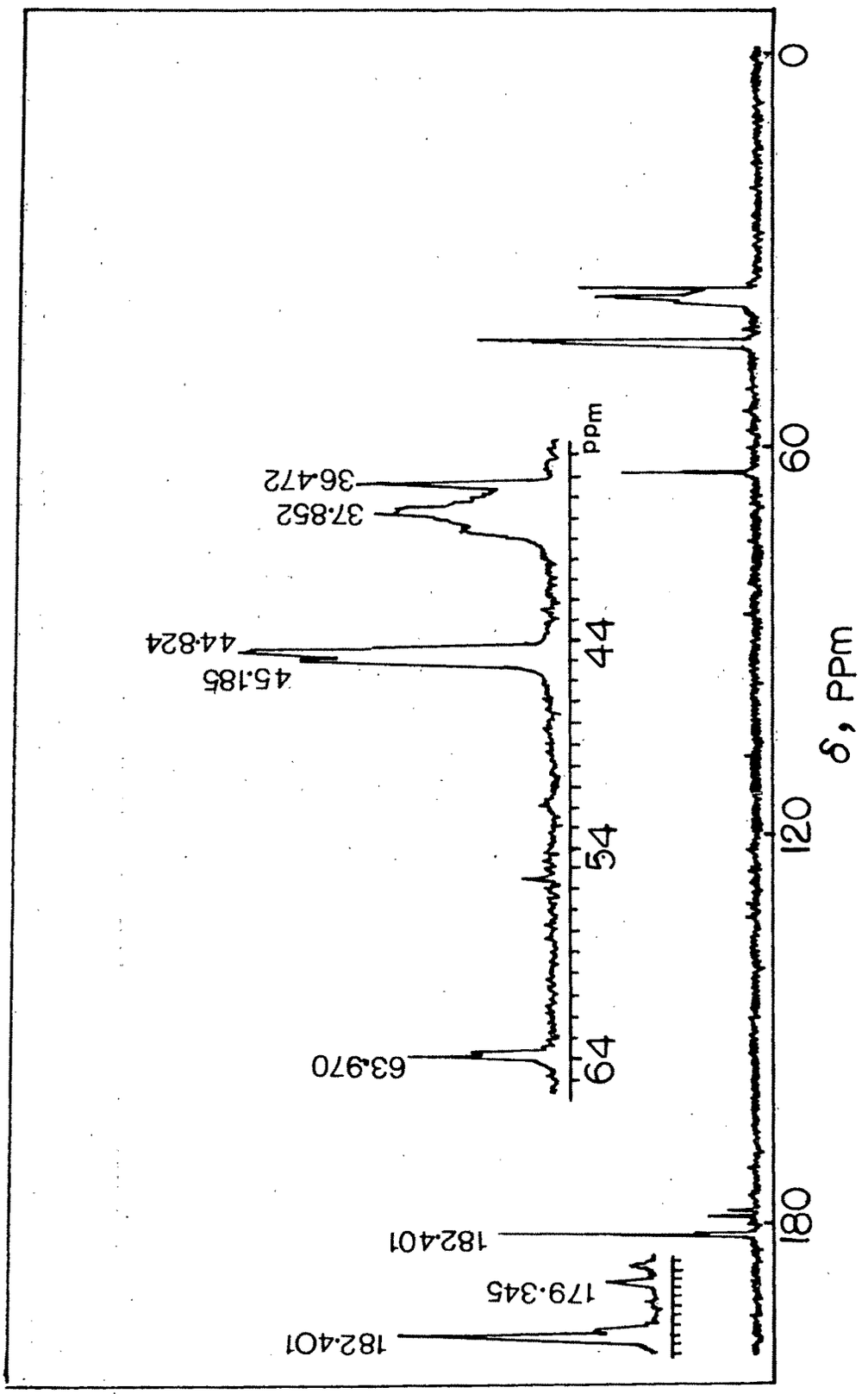

Fig. 20 : 13C-NMR spectra of P(AA-AAc) 65:35 copolymer.

iii) Reactivity Ratios :

The experimental feed ratios of various monomers as well as the composition of the resulting copolymers are obtained from elemental analysis. Generally the compositional analysis of acrylamide copolymers is based on nitrogen analysis[299]. The values are summarized in Table 1. From these values, it can be seen that the values in the feed is generally higher than the experimental compositions in case of the copolymers.

The reactivity ratios were estimated for the copolymer series prepared using the elemental analysis composition. The change in composition of the copolymer in the copolymerization of two monomers is expressed as :

$$\frac{dM_1}{dM_2} = \frac{M_1}{M_2} \frac{r_1M_1 + M_2}{r_2M_2 + M_1}$$

where M_1 and M_2 are the concentration of monomers, $r_1 = k_{11} / k_{12}$ and $r_2 = k_{22}/k_{21}$ are the monomer reactivity ratios. At low conversion rate (dM_1/dM_2) corresponds to M_1/M_2.

Introducing

$$M_1 / M_2 = X \text{ and } dM_1 / dM_2 = Y$$

the composition equation can be written as

$$Y = X \frac{r_1X + 1}{r_2 + X}$$

By rearranging the above equation

$$\frac{X}{Y}(Y\text{-}1) = \frac{r_1 X^2}{Y} - r_2$$

Table 1 : Composition of acrylamide and acrylic acid in feed and in copolymers.

Sample	Mole Fraction of AA in Feed (M_1)	Elemental Analysis N (%)	Mole Fraction in AA in Copolymer (Φ_1)
AA-AAc (50:50)	0.504	8.66	0.44
AA-AAc (65:35)	0.653	10.16	0.52
AA-AAc (85:15)	0.852	14.86	0.76

This equation was modified by Finemann-Ross[300] (F-R) as

$$G = r_1 F - r_2 \text{ or } \frac{G}{F} = -r_2 \frac{1}{F} + r_1$$

$$\text{Where } G = \frac{X(Y-1)}{Y} \text{ and } F = \frac{X^2}{Y}$$

On plotting X (Y-1)/Y against X^2 / Y a straight line was obtained, whose slope was r_1 and the intercept yielded r_2.

In this method the data obtained under extreme experimental conditions i.e. at very low M_2 and at very low M_1 comonomer concentrations, have the greatest influence on the slope of line calculated by the usual linear least square procedure. The r_1 and r_2 values depend on factors like which monomer is selected M_1. Hence, to remove such difficulties this method was further developed by Kelen-Tudos[301] (K-T) (see Table 2) which considers the term ε

$$\therefore \frac{G}{\varepsilon + F} = \left[r_1 + \frac{r_2}{\varepsilon} \right] \frac{F}{\varepsilon + F} - \frac{r_2}{\varepsilon}$$

where ε is an arbitrary constant (ε >0). Generally ε value is chosen with regard to entire experimental range of composition for both the polymers and comonomers. Of all the F values calculated, if F_m stands for the lowest and F_M stands for the highest value then

$$\varepsilon = (F_M . F_m)^{1/2}$$

Table 2 : Kelen-Tudos parameters.

Sample	$X = \frac{M_1}{M_2}$	$Y = \frac{\Phi_1}{\Phi_2}$	$G = X\frac{(Y-1)}{Y}$	$F = \frac{X^2}{Y}$	$\xi = \frac{F}{(\varepsilon + F)}$	$\theta = \frac{G}{(\varepsilon + F)}$
AA-AAc (50:50)	1.01	0.80	-0.26	1.29	0.26	-0.05
AA-AAc (65:35)	1.88	1.08	0.14	3.29	0.47	0.019
AA-AAc (85:15)	5.75	3.10	3.90	10.64	0.74	0.27

$\varepsilon = (F_{min} F_{max})^{1/2} = 3.71$; M_2 is the mole fraction of acrylic acid in feed, Φ_1 and Φ_2 are the mole fractions of acrylamide and acrylic acid in the copolymer.

By introducing

$$\theta = \frac{G}{\varepsilon + F} \text{ and } \xi = \frac{F}{\varepsilon + F}$$

$$\text{then, } \theta = r_1 + \frac{r_2}{\varepsilon}\,\xi - \frac{r_2}{\varepsilon}$$

$$\text{or } \theta = r_1\,\xi - \frac{r_2}{\varepsilon}(1-\xi)$$

On plotting θ values calculated from the experimental data as a function ξ a straight line is obtained which when extrapolated to ξ = 0 and ξ = 1 gives - r_2/ε and r_1 values. In this equation by introducing the ε term and proper choice of ε, ensures uniform distribution of experimental points along the interval (0,1) and removes discrepancies in r_1 and r_2 values. The reactivity ratios r_1 and r_2 are for monomer-1 (acrylamide) and monomer-2 (acrylic acid) respectively. The F-R method gives values of r_1 and r_2 as 0.463 and 1.092 respectively. The values obtained for r_1 and r_2 from the K-T method are 0.427 and 0.945 respectively. Several values of r_1 and r_2 are reported for the same two monomers in literature[302,303] depending on temperature and reaction conditions.

Using information on the reactivity ratios the statistical distribution of the monomer sequences M_1-M_1, M_2-M_2 and M_1-M_2 was calculated[304]. The fractions of M_1-M_1, M_2-M_2 and M_1-M_2 bond in a copolymer is represented as X', Y' and Z' respectively.

$$\begin{aligned} X' &= a_1 / a_1 + a_2 + a_3 \\ Y' &= a_2 / a_1 + a_2 + a_3 \qquad \text{..... (1)} \\ Z' &= a_3 / a_1 + a_2 + a_3 \end{aligned}$$

where a_1, a_2 and a_3 are total number of M_1-M_1, M_2-M_2 and M_1-M_2 bond in a copolymer molecule. If X', Y' and Z' are represented by a triangular system then each apex of a triangle corresponds to a homopolymer A and B and a perfectly alternating copolymer C.

In case of a random copolymer the probability of occurrence of a sequence of the same monomer units M_1 of length n is given by

$$P(n)_{M_1} = P_{11}^{\,n-1} (1-P_{11}) \qquad \text{.....(2)}$$

where P_{11} is the probability for a monomer of the type M_1 to join the other monomer of type M_1. Similarly for M_2

$$P(n)_{M_2} = P_{22}^{\,n-1} (1-P_{22}) \qquad \text{.....(3)}$$

If the total number of blocks composed of M_1 and M_2 units are designated by N_1 and N_2 then

$$\sum_{n=1}^{\infty} n N_1 P(n)_{M_1} = \Phi_1 N \qquad \text{.....(4)}$$

and

$$\sum_{n=1}^{\infty} n N_2 P(n)_{M_2} = (1-\Phi_1) N \qquad \text{.....(5)}$$

where N is the degree of polymerization of a large chain molecule, Φ_1 is the mole fraction of M_1 in the copolymer. Using equations (2) - (5)

$$N_1 = (1-P_{11}) \Phi_1 N \qquad \text{.....(6)}$$

and

$$N_2 = (1-P_{22}) (1-\Phi_1) N \qquad \text{.....(7)}$$

a_1 and a_2 which is the total number of M_1-M_1 and M_2-M_2 unit in a copolymer sequence, then a_1 and a_2 are calculated as follows for a random copolymer -

$$a_1 = \sum_{n=2}^{\infty} (n-1) N_1 P(n)_{M_1} = N_1 P_{11} / (1-P_{11}) \qquad \text{.....(8)}$$

$$a_2 = \sum_{n=2}^{\infty} (n-1) N_2 P(n)_{M_2} = N_2 P_{22} / (1-P_{22}) \qquad \text{.....(9)}$$

Substituting equation (6) and (7) in the above equations

$$a_1 = P_{11}\,\Phi_1\,N \qquad \text{.....(8')}$$

$$a_2 = P_{22}\,(1-\Phi_1)\,N \qquad \text{.....(9')}$$

If the degree of polymerization is taken as N, then $a_1 + a_2 + a_3 = N\text{-}1$ and we have

$$a_3 = (1-P_{11})\,\Phi_1\,N + (1-P_{22})\,(1-\Phi_1)\,N\text{-}1 \qquad \text{.....(10)}$$

From equations (1), (8'), (9') and (10) we get -

$$X' = P_{11}\,\Phi_1\,N / N\text{-}1 \cong P_{11}\,\Phi_1$$

$$Y' = P_{22}\,(1-\Phi_1)\,N / N\text{-}1 \cong P_{22}\,(1-\Phi_1)$$

$$Z' = \left\{[(1-P_{11})\,\Phi_1 + (1-P_{22})\,(1-\Phi_1)]\,N\text{-}1\right\} \;/\; N\text{-}1$$

$$= (1-P_{11})\,\Phi_1 + (1-P_{22})\,(1-\Phi_1)$$

For an ordinary copolymer P_{11} and P_{22} are expressed as follows

$$P_{11} = r_1 f_1 / (r_1 f_1 + 1)$$

$$P_{22} = r_2 / (r_2 + f_1)$$

where r_1 and r_2 are the monomer reactivity ratios and f_1 is the mole ratio of M_1 and M_2 in the feed. The relation between Φ_1 and f_1 is given by

$$f_1 = \left\{2\Phi_1 - 1 + [(2\Phi_1\text{-}1)^2 + 4\,r_1\,r_2\,\Phi_1\,(1-\Phi_1)]^{1/2}\right\} \;/\; 2r_1\,(1-\Phi_1)$$

Using this equation the above equations can be rewritten as

$$P_{11} = 1\text{-}2\,(1-\Phi_1) \,/\, \left\{1 + [(2\Phi_1 - 1)^2 + 4\,r_1\,r_2\,\Phi_1\,(1-\Phi_1)]^{1/2}\right\}$$

and

$$P_{22} = 1\text{-}2\Phi_1 \,/\, \left\{1 + [(2\Phi_1 - 1)^2 + 4\,r_1\,r_2\,\Phi_1\,(1-\Phi_1)]^{1/2}\right\}$$

From these equations, the final equations obtained are -

$$X' = \Phi_1 - 2\Phi_1 (1-\Phi_1) / \{1 + [(2\Phi_1-1)^2 + 4 r_1 r_2 \Phi_1 (1-\Phi_1)]^{1/2}\}$$

$$Y' = (1-\Phi_1) - 2 \Phi_1 (1-\Phi_1) / \{1 + [(2\Phi_1 - 1)^2 + 4 r_1 r_2 \Phi_1 (1-\Phi_1)]^{1/2}\}$$

$$Z' = 4 \Phi_1 (1-\Phi_1) / \{1 + [(2 \Phi_1 - 1)^2 + 4 r_1 r_2 (1-\Phi_1)]^{1/2}\}$$

Using a graphical triangular co-ordinate system the alternation tendency or blockiness of a copolymer system can be calculated. When $r_1 r_2$ is large, blockiness is large and inversely when $r_1 r_2$ is small, alternation is large for the copolymers of the same compositions. Φ_1 is the mole fraction of acrylamide in the copolymer obtained from elemental analysis data. The mean sequence lengths χ_{AA} and χ_{AAc} were then calculated using the relations[297]

$$\chi_{AA} = 1 + r_1 [\Phi_1] / [\Phi_2]$$

$$\chi_{AAc} = 1 + r_2 [\Phi_2] / [\Phi_1]$$

The intermonomer linkages and mean sequence length distributions for the AA-AAc copolymers are listed in Table 3. For a series of AA-AAc copolymers, χ_{AA} varied from 1.3 at 0.44 / 0.56 mole ratio of AA/AAc in the copolymer to 2.4 with 0.76 / 0.24 mole ratio. The calculated mole fraction of AA-AAc linkages in each polymer is relatively high indicating an alternating tendency.

iv) Thermogravimetric Analysis :

TGA of PAA, PAAc and the copolymers (50:50) systems are given in Fig. 21. The thermogram of the copolymer falls in between those of the corresponding homopolymers, implying that the thermal stability of the copolymers is between the two homopolymers. Two stage decomposition was observed for all the polymers except PAA. TGA of PAA showed three stage decomposition which was observed earlier also[305]. First stage is the loss of water, which is non-stoichiometric. This is followed by subsequent loss of ammonia and other gaseous products from the

Table 3 : Structural data for the copolymers of AA and AAc.

Sample	Composition[a] (mole fraction)		Blockiness[b] (mole fraction)		Alteration[b] (mole fraction)	Mean Sequence length[c]		
	AA (Φ_1)	AAc (Φ_2)	AA-AAc (X')	AAc-AAc (Y')	AA-AAc (Z')	χ_{AA}	χ_{AAc}	χ_{AA}/χ_{AAc}
AA-AAc (50:50)	0.44	0.56	0.140	0.260	0.600	1.3	2.2	0.6
AA-AAc (65:35)	0.52	0.48	0.215	0.175	0.610	1.5	1.9	0.8
AA-AAc (85:15)	0.76	0.24	0.552	0.032	0.417	2.4	1.3	1.8

a - From elemental analysis

b - Statistically calculated using reactivity ratios (see ref. 297)

c - Using Kelen-Tudos reactivity ratio

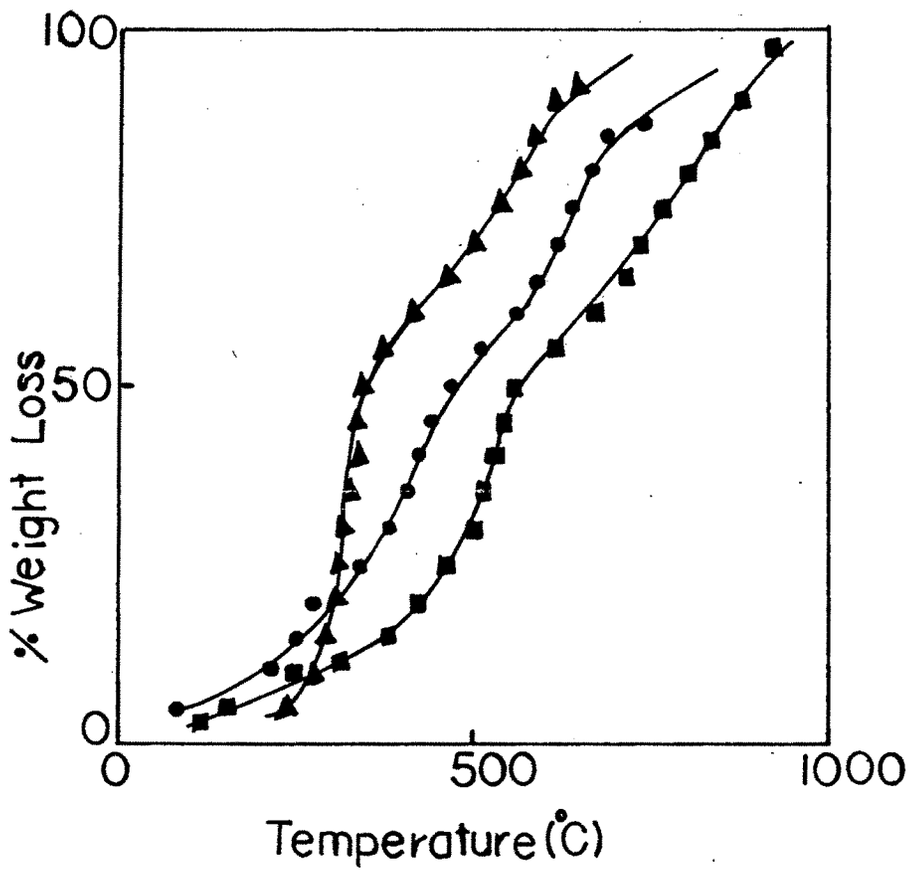

Fig. 21 : TGA curves of polyacrylamide, P(AA-AAc) 50:50 copolymer and polyacrylic acid at a heating rate of 10 K min^{-1} in air.

polyacrylonitrile structure formed during decomposition of PAA and partly from the remaining PAA in the course of heating upto 600°C[306]. In case of PAAc, the first stage decomposition started at ~ 240°C. This is due to formation of anhydride linkages.

Similar values were reported for PAAc earlier[307]. Heating above 300-350°C results in rapid decomposition to monomers CO_2 and volatile hydrocarbons. The activation energy (E) of decomposition of polymers were evaluated using various equations from the experimental results. The activation energy associated with each stage of decomposition was also evaluated by the well known Broido's method[308-310]. The equation used for the calculation of activation energy (E) was

$$\ln \ln (1/y) = (-E/R)(1/T) + \text{constant}$$

where $y = (W_t - W_\alpha) / (W_o - W_\alpha)$, where y is the fraction of the number of initial molecules not yet decomposed, W_t is the weight at any time t, W_α is the weight at infinite time (=zero) and W_o is the initial weight. A plot of ln ln (1/y) versus 1/T as seen from Fig. 22 relating to above equation gives an excellent approximation to a straight line over a range of $0.999 < y < 0.001$. The slope is related to the activation energy. The activation energy values obtained are listed in Table 4.

A method which uses a single heating rate was the vanKrevelen[311] method. This method makes use of the following equation

$$\ln \left| \ln (1-C) \right| = \frac{E}{R (T_m + 1)} \ln T$$

where $C = W_o - W_t / Wo$ and T_m is the temperature at maximum conversion rate dW/dt. From the corresponding linear plot E values can be evaluated. Another method - the Ozawa[312] method, a dynamic analysis technique, was also used to evaluate the activation energy. Thermograms were recorded at various heating rates of 10, 15 and

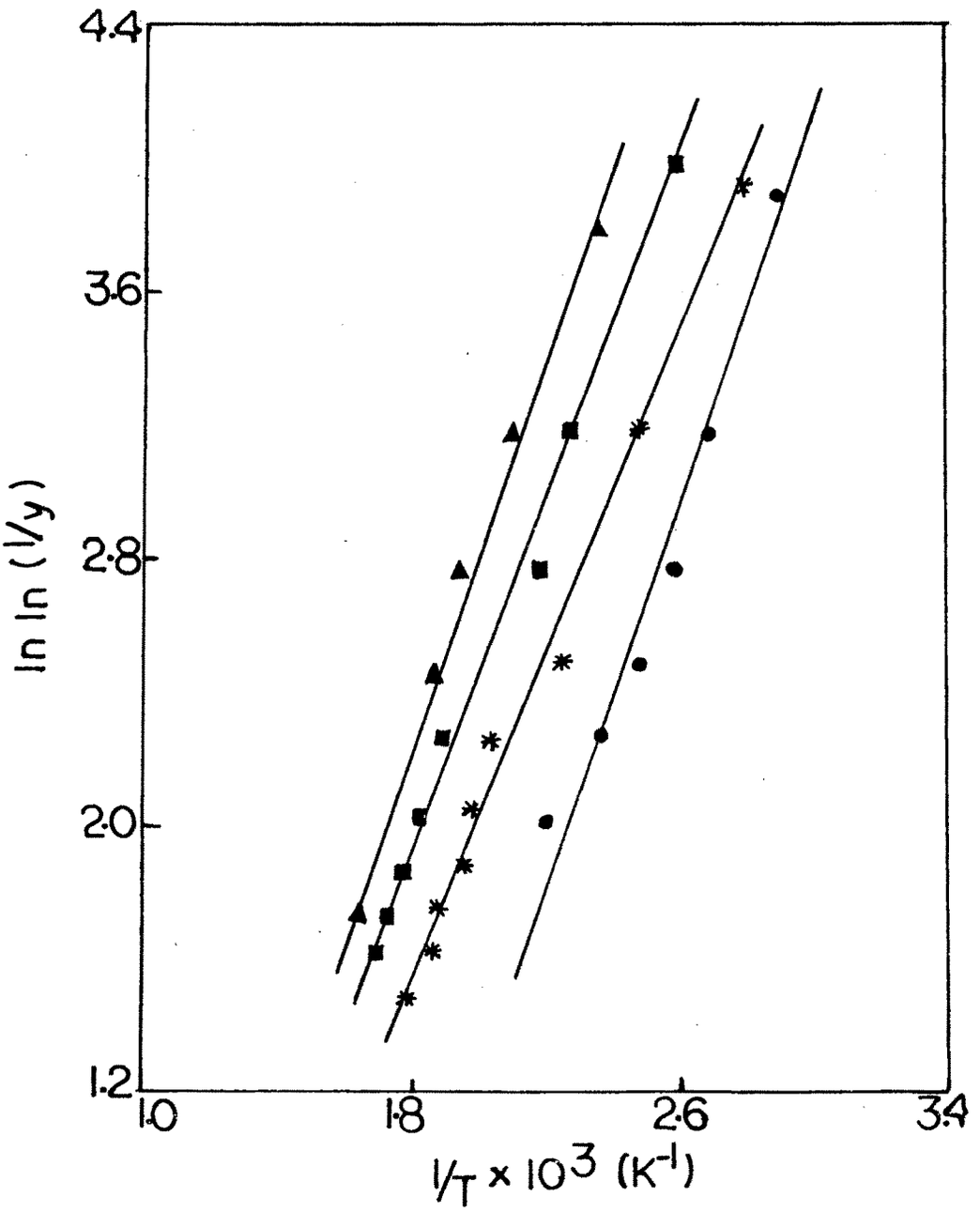

Fig. 22 : Plot of ln ln (1/Y) vs. 1/T for ● PAA; ■ P(AA-AAc) 85:15 copolymer; ✱ P(AA-AAc) 50:50 copolymer; ▲ PAAc.

20 K min^{-1} in air. The fraction of decomposition Q was evaluated from the following equation

$$Q = (W_o - W_t) / (W_o - W_f)$$

where W_o is the initial weight of polymer, W_t is the weight of the polymer at temperature t, and W_f is the final weight. (1-Q) values were found for each heating rate from the TG curves; (1-Q) values obtained were plotted against 1/T. According to Ozawa's method[312,313], the plot of log β (where β is the heating rate) against the reciprocal of absolute temperature for different values of (1-Q) is linear. The activation energy of decomposition was obtained from the slope of the above linear plot, using the equation

$$\text{Slope} = -0.4567\ (E/R)$$

The representative plot of log β versus 1/T, for PAA system at different values of (1-Q) each differing by 0.05 is shown in Fig. 23. The activation energy values are given in Table 4. The activation energy of decomposition varied with (1-Q) and were not exactly constant. The activation energy values of decomposition for PAA in N_2 atmosphere was 157.5 ± 1.71. This indicates higher stability of PAA in nitrogen atmosphere as expected[314].

The Reich[315] method also makes use of multiple heating rates. Reich proposed the following equation

$$E = 2.303\ R \log [(B_2/B_1)\ (T_1/T_2)^2] / (1/T_1 - 1/T_2)$$

where B_1 and B_2 are different heating rates, T_1 and T_2 are temperatures for each heating rate for a given amount of decomposition obtained from TG curves. A comparison of the activation energy values evaluated by different methods are listed in Table 4.

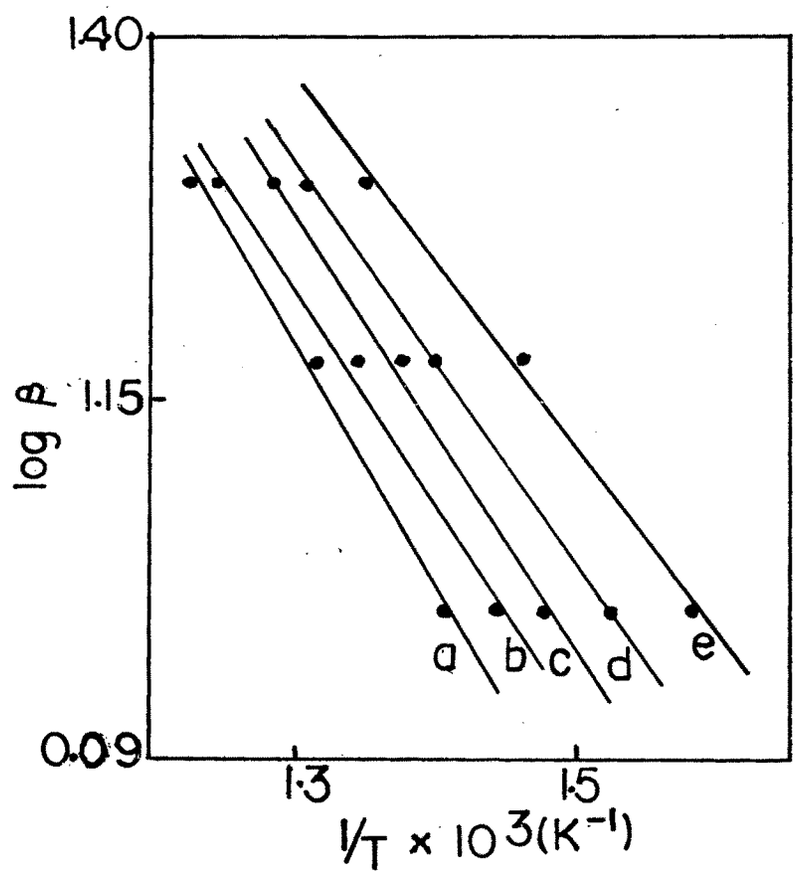

Fig. 23 : Representative of log β vs. 1/T for polyacrylamide. Values of (1-α) are (a) 0.50; (b) 0.55; (c) 0.60; (d) 0.65; (e) 0.70. β is the heating rate (K min^{-1}).

Table 4 : Activation energy of decomposition using different equations and fusion temperature and enthalpy change values.

Polymer Systems	Activation Energy (E_a) kJ mol^{-1}				Phase Transition Temperature (°C)	Enthalpy Change (J g^{-1})
	Broido[a]	van Kravelen[a]	Ozawa	Reich		
PAA	25.6 22.9	27.4 23.4	27.9	24.7	84.8	461.8
P(AA-AAc) 85:15	19.1 34.8	21.7 36.8	83.5	81.1	a) 178.4 b) 228.8	a) 26.8 b) 218.1
P(AA-AAc) 65:35	17.1 36.1	21.5 36.7	82.4	83.5	a) 173.6 b) 226.1	a) 1.2 b) 108.5
P(AA-AAc) 50:50	20.3 20.7	21.3 22.1	--	--	a) 168.7 b) 228.4	a) 1.7 b) 67.6
PAAc	8.9 2.9	8.9 2.3	51.5	49.7	a) 116.1 b) 236.1	a) 60.5 b) 486.1

a - Calculated at a heating rate of 10 K min^{-1}, in air.

v) Differential Scanning Calorimetry :

DSC curves of PAAc, PAA and copolymers are shown in Fig. 24-28. Values of glass transition temperature Tg for PAAc in literature are 106°C[316], 130°C[317] and 180°C[318]. The Tg of PAAc increases with increasing anhydride concentration, which occurs primarily by intramolecular reactions. Decarboxylation also occurs simultaneously with water elimination, but at a much slower rate[319]. DSC of PAAc is shown in Fig. 28 which shows a Tg at 110°C and the enthalpy change associated with it as 60.5 Jg^{-1}. Melting temperature Tm of PAAc was 250°C and the enthalpy change associated with it was 486 Jg^{-1} [320]. Tg of PAA was observed at 84.8°C and the onset of softening temperature occured at ~ 190°C. Reported values were 153°C and 210°C respectively[321]. Copolymers showed an enhancement in Tg values as seen from Table 4 due to specific interactions between acrylamide and acrylic acid moieties.

Viscosity Studies :

The viscosity of solutions of PAA, the copolymers and PAAc were studied at different temperatures of 35, 40 and 45°C. The studies were carried out in aqueous medium and in presence of various concentrations of different electrolytes. Intrinsic viscosity was calculated using the Huggins and Kraemer equations[286]

$$\eta_{sp} / C = [\eta] + K` [\eta]^2 C$$

$$\ln \eta_r / C = [\eta] - K`` [\eta]^2 C$$

where K` and K``are constants for a given polymer / solvent / temperature system. For many linear flexible polymer systems, K` often indicates the measure of the solvent power; the poorer the solvent higher the value of K`. The K`-K`` values were found to be ~ 0.5 as expected[322,323]. Intrinsic viscosities of the different systems and the temperatures studied and the values of K`-K`` are given in Table 5.

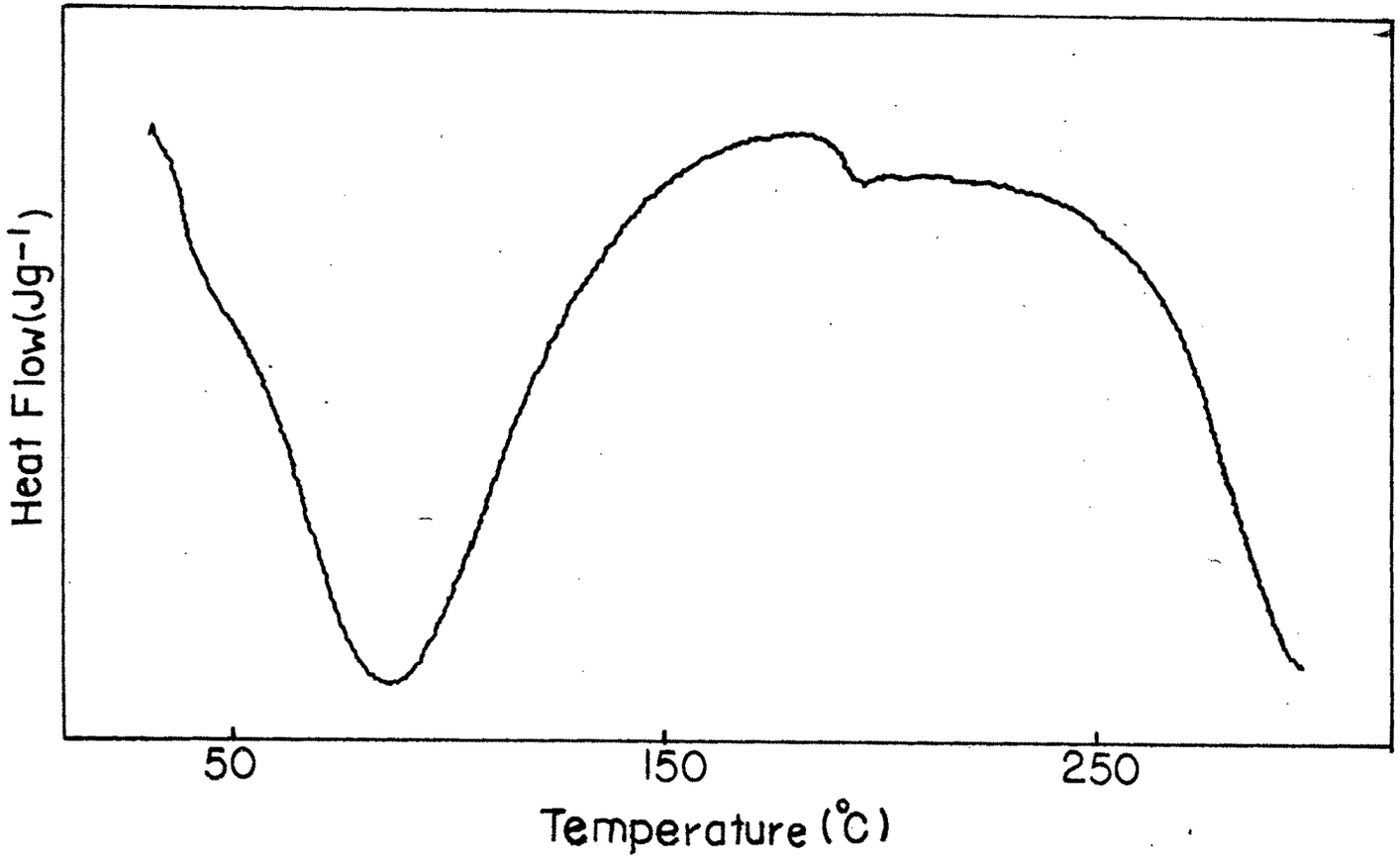

Fig. 24 : DSC curve of polyacrylamide.

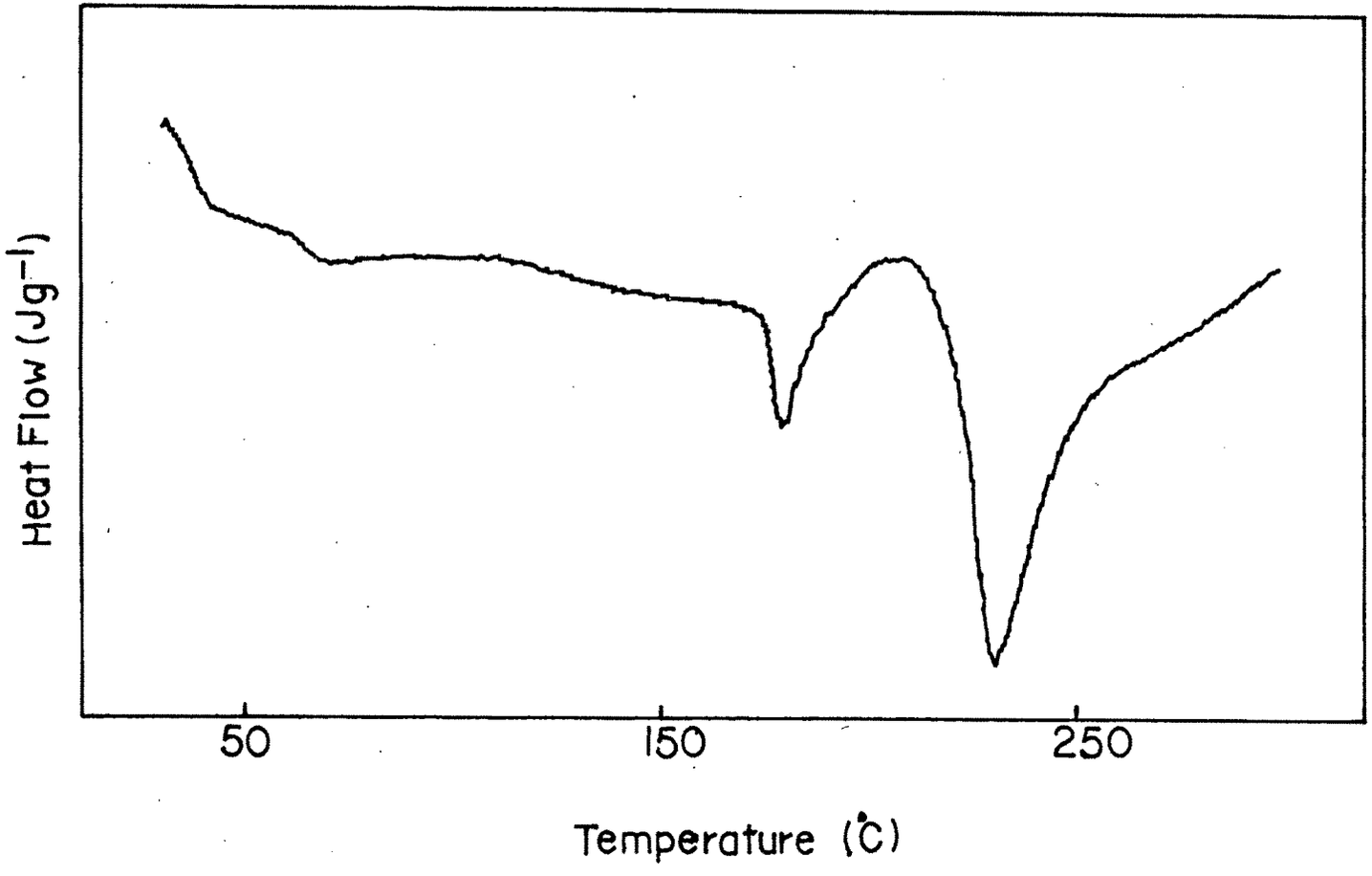

Fig. 25 : DSC curve of P(AA-AAc) 85:15 copolymer.

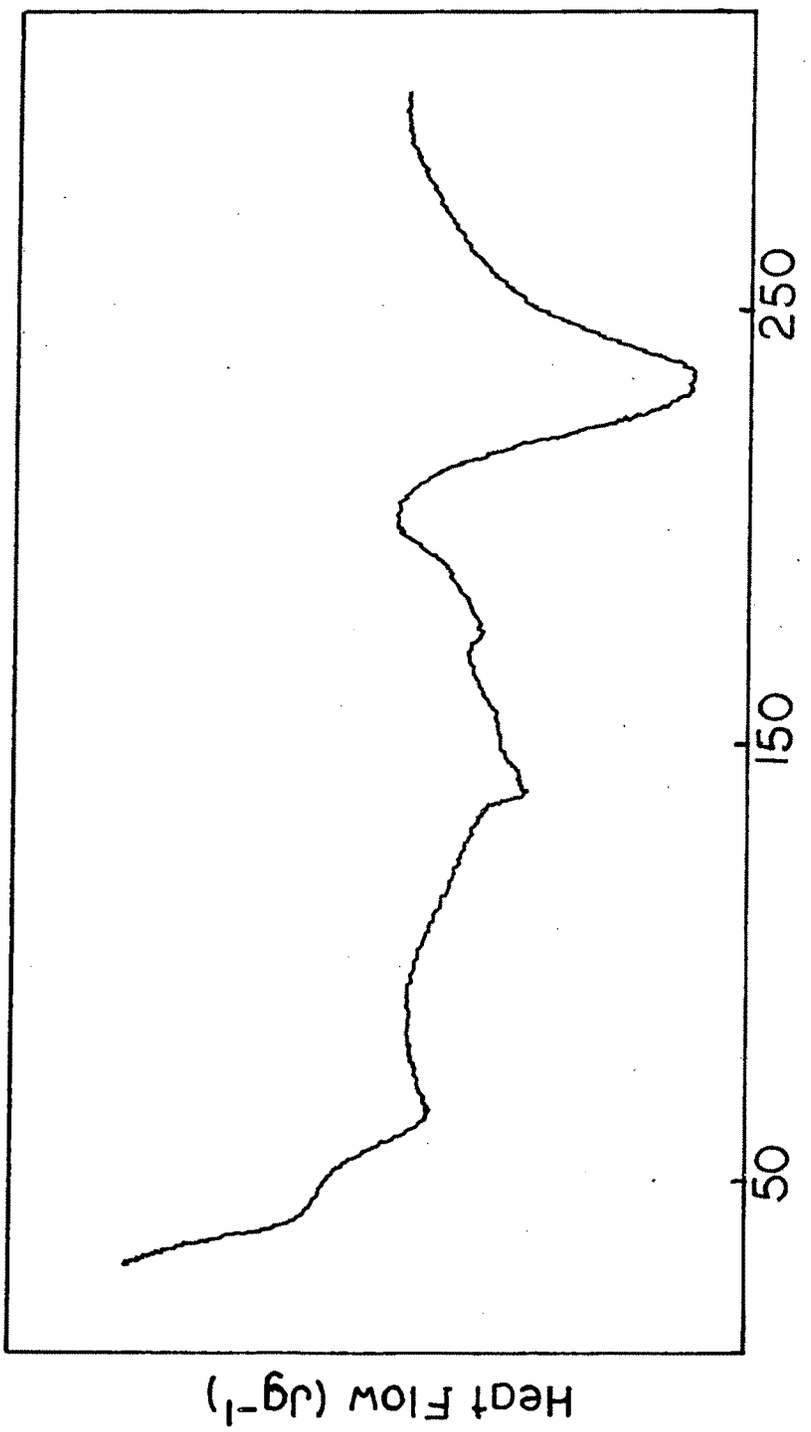

Fig. 26 : DSC curve of P(AA-AAc) 65:35 copolymer.

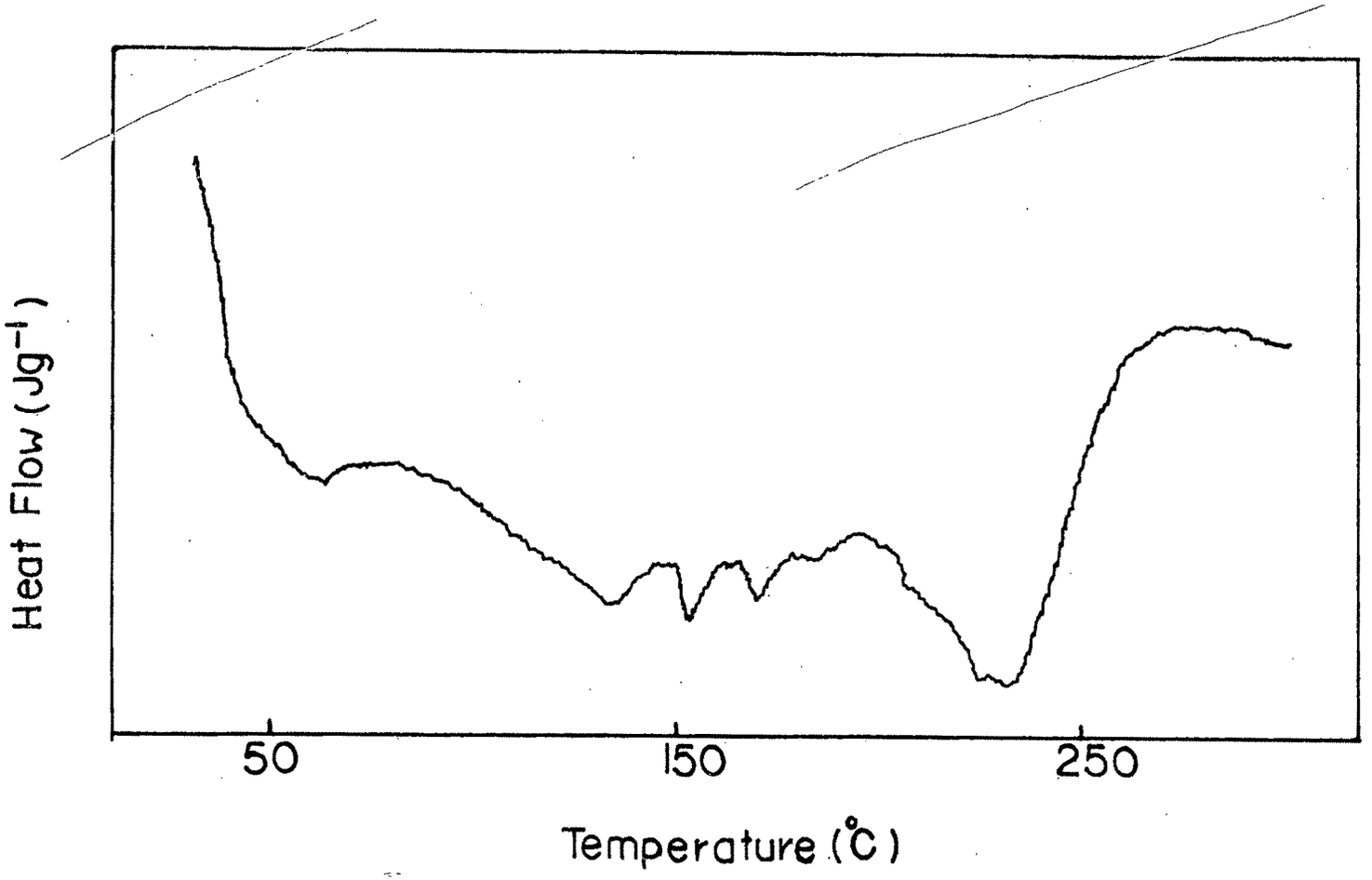

Fig. 27 : DSC curve of P(AA-AAc) 50:50 copolymer.

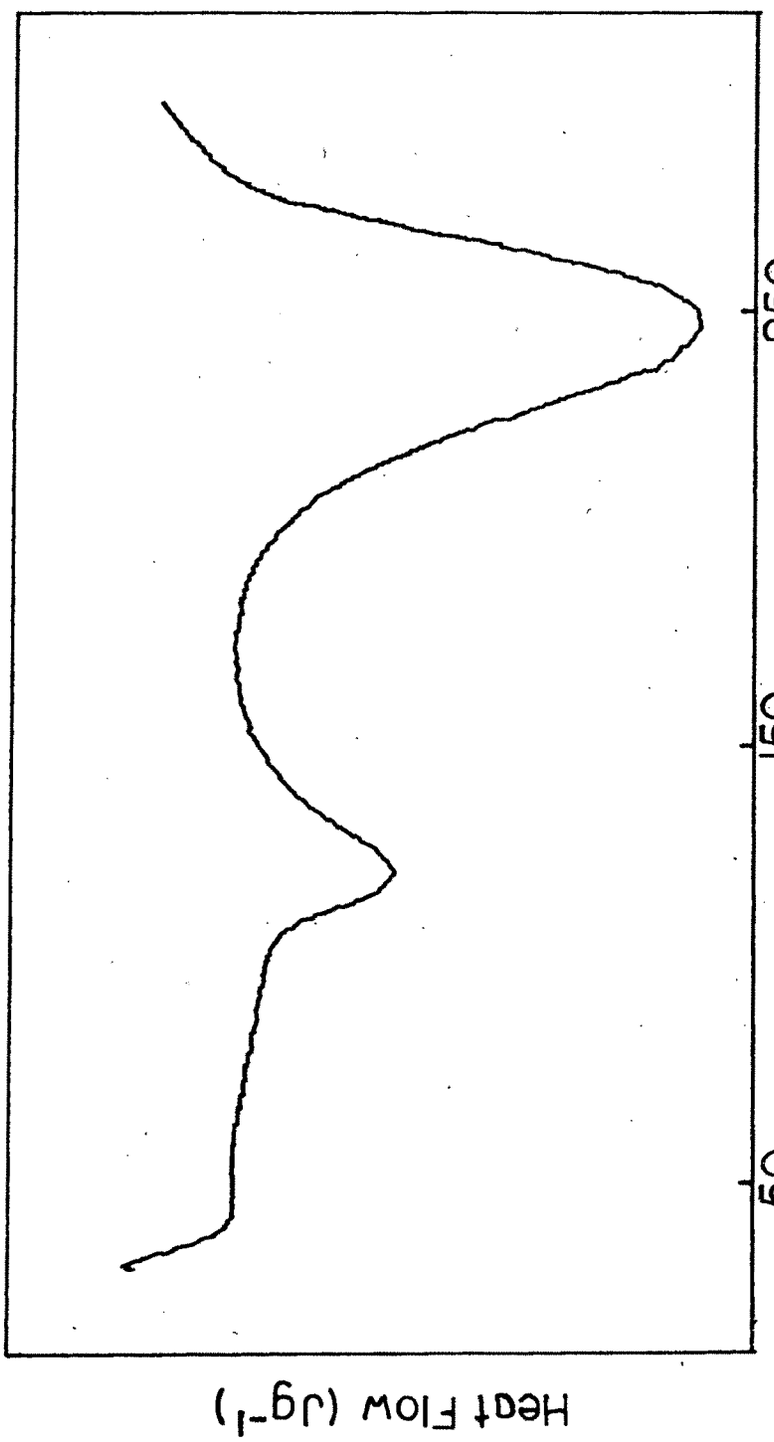

Fig. 28 : DSC curve of polyacrylic acid.

Table 5 : Intrinsic viscosities of various polymer systems at different temperatures in aqueous solution.

Polymer System / Solvent	Intrinsic Viscosity [η] (dl g^{-1})			K`-K``		
	35°C	40°C	45°C	30°C	35°C	40°C
PAA/H_2O	2.98	2.91	2.62	0.48	0.51	0.51
PA/0.05M $NaNO_3$	3.85	3.68	3.40	0.50	0.51	0.50
PAA/0.3M $NaNO_3$	3.87	3.67	3.58	0.50	0.50	0.51
PAA/0.5M $NaNO_3$	3.75	3.91	3.94	0.51	0.50	0.51
PAA/0.1M Al $(NO_3)_3$	4.00	3.74	3.56	0.49	0.51	0.50
PAA/0.3M Al $(NO_3)_3$	3.97	4.04	4.53	0.48	0.50	0.46
PAA/0.5M Al $(NO_3)_3$	4.10	4.19	4.23	0.50	0.50	0.51
P(AA-AAc) 85:15/H_2O*	26.4	32.6	38.9	--	--	--
P(AA-AAc) 85:15/0.3M $NaNO_3$	2.60	2.77	3.07	0.48	0.51	0.50
P(AA-AAc) 85:15/0.5M $NaNO_3$	2.36	2.73	2.92	0.50	0.47	0.51
P(AA-AAc) 65:35/H_2O*	26.2	31.6	39.8	--	--	--
P(AA-AAc) 65:35/0.05M $NaNO_3$	1.52	1.62	1.74	0.48	0.51	0.50
P(AA-AAc) 65:35/0.1M $NaNO_3$	1.52	1.54	1.66	0.47	0.49	0.52
P(AA-AAc) 65:35/0.5M $NaNO_3$	1.53	1.54	1.58	0.49	0.50	0.51
P(AA-AAc) 50:50/H_2O*	7.1	8.9	11.2	--	--	--
PAAc/H_2O*	23.6	28.4	33.5	--	--	--

*These systems behaved as polyelecrolytes and hence K`-K`` could not be computed.

Some representative plots are shown in Fig. 29-30. The variation of [η] with temperature depended on salt concentration. [η] of PAA in H_2O and in presence of lower concentrations of electrolytes [$NaNO_3$ and $Al(NO_3)_3$] showed a decrease with increase in temperature. Other systems showed an increase in [η] with increase in temperature. On initial addition of the salt, the structure of water breaks and due to the solvation of the electrolyte ions, the polymer chains get dehydrated and as a result with increasing temperature more coiling of the polymer chains occur and hence [η] values decreases whereas due to electrolytic repulsions between the electrolyte molecules that are surrounding the polymer chains, the [η] values increase with increase in temperature at higher electrolyte concentrations. The decrease in [η] with increasing temperature indicates a decrease in hydrodynamic volume of polymer molecules. This is due to conformational and solvent association changes with increasing temperature[324,325]. Increase in temperature of a polymer solution generates two antagonistic effects[324,326]. First, increase in temperature generally leads to an increase in solvent power, i.e. solubility of the polymer in a solvent increases. This results in uncoiling of the polymer chains, leading to increase in [η] with temperature. Second, increase in temperature may lower the rotational barrier, thereby enhancing the degree of rotation about a skeletal bond, forcing the molecular chains to assume a more compact coiled configuration. This leads to a decrease in [η] with increase in temperature. The decrease in [η] with increase in temperature was observed earlier also for various acrylamide based copolymers[297] whereas, polyelectrolytes like PAAc show an increase in [η] with increasing temperature[289].The effect of different concentrations of $NaNO_3$ on the viscosity behaviour of PAA is different from that on the viscosity behaviour of AA-AAc copolymer. [η] of PAA shows a maximum when plotted against the ionic strength of $NaNO_3$ (Fig. 31). This behaviour of acrylamide based copolymers was observed earlier also[297]. [η] of AA-AAc copolymer, (65 : 35) varied linearly with reciprocal square root of ionic strength i.e. $I^{-1/2}$ (Fig. 31). This behaviour was observed for polyelectrolytes by a number of workers[296,327,328].

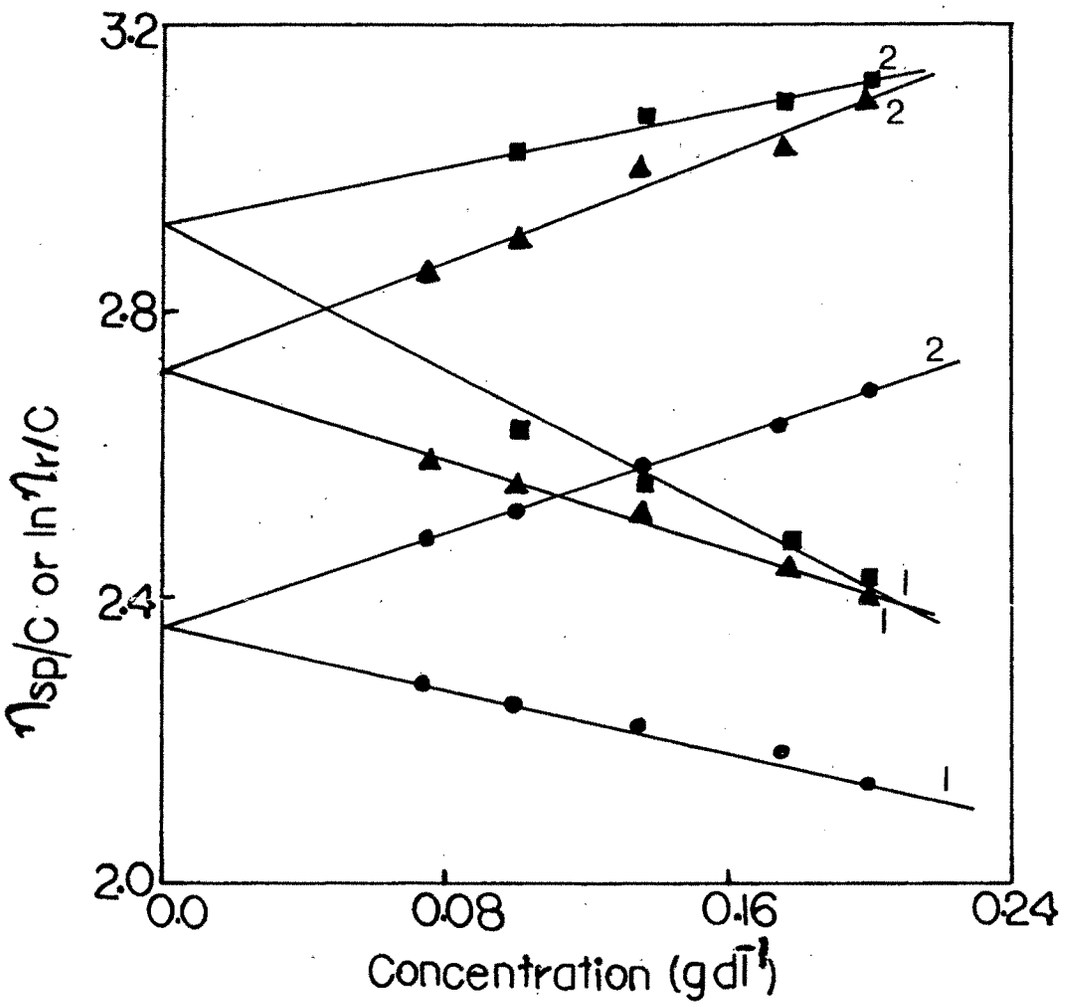

Fig. 29 : Plots of (1) ln η_r/C; (2) η_{sp}/C for the P(AA-AAc) 85:15 / 0.5M $NaNO_3$ system. ● 35°C; ▲ 40°C; ■ 45°C.

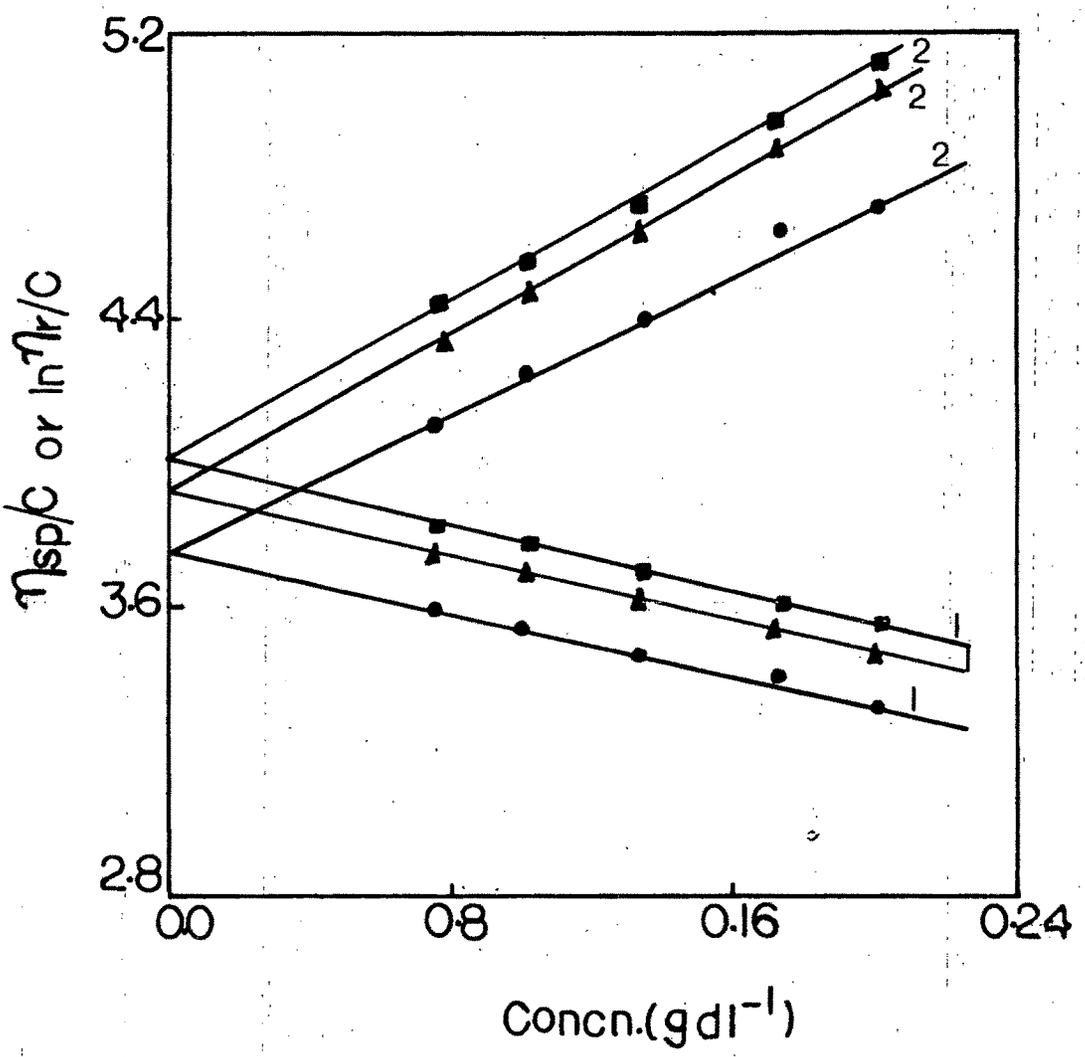

Fig. 30 : Plots of (1) ln η_r/C; (2) η_{sp}/C for PAA / 0.5M $NaNO_3$ system.
● 35°C; ▲ 40°C; ■ 45°C.

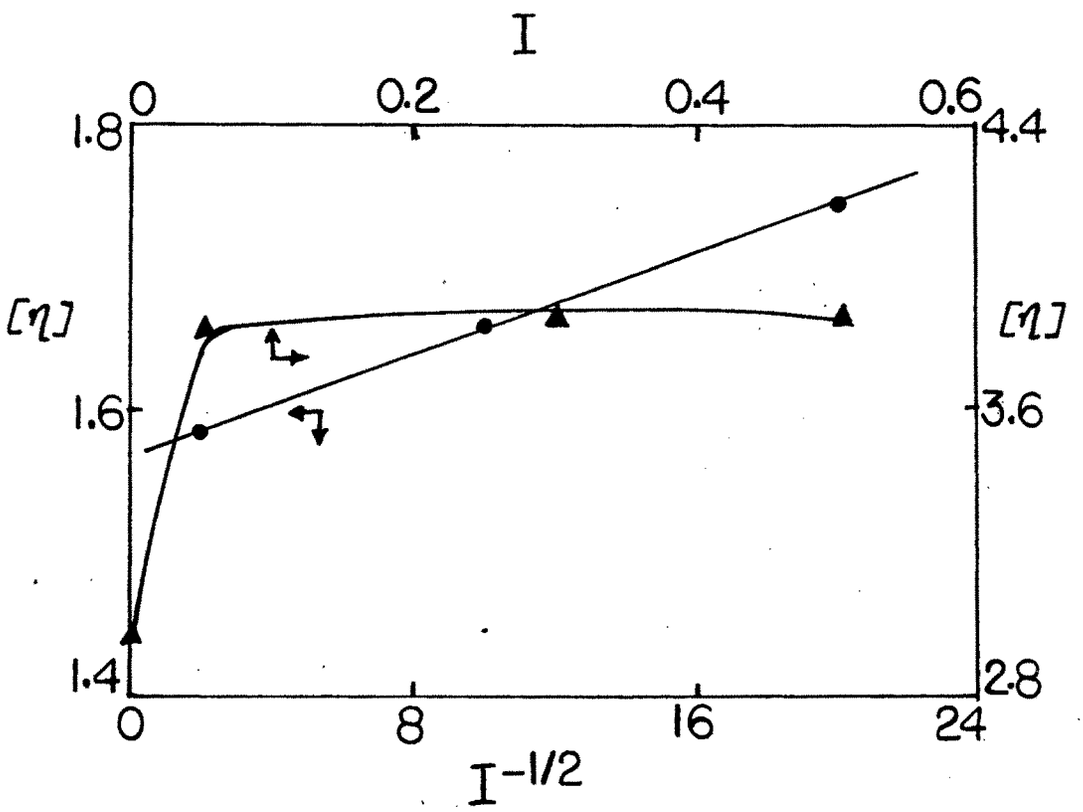

Fig. 31 : Plot of (●) $I^{-½}$ vs. [η] for (AA-AAc) 65:35 copolymer / NaNO3 at 40°C and (▲) I vs [η] PAA / $NaNO_3$ at 35°C.

This indicates that copolymers having acrylic acid as a comonomer act as polyelectrolytes in aqueous media. There is an electrical double layer at the solid-liquid interface (i.e. at the polyion-solvent interface). The double layer thickness at the polyion-solvent interface decreases with the addition of an electrolyte. Hence, there is less overlapping of the double layers and consequently less viscosity with increase in concentration of salt.

The viscosities of copolymers P(AA-AAc) - 50:50, 65:35, 85:15 and PAAc in water, like other polyelectrolytes showed an unique dependence on concentration. η_{sp}/C for the above mentioned polymers in water increases with dilution, contrary to the behaviour of nonionic polymers. Representative plots are shown in Fig. 32. As the solution is diluted, the polymer molecules no longer fill all of the space and intervening regions extract some of the mobile ions. Net charges develop in the domain of polymer molecules, causing them to expand. As this process continues with further dilution, the expansive forces increase. At high dilutions, the polymer molecules loose most of their mobile ions and are extended virtually to their maximum length[329]. This leads to high values of η_{sp}/C. Such data can be satisfactorily handled through the use of the empirical relation i.e. the Fuoss and Strauss equation[330]

$$\eta_{sp}/C = A'/(1 + B'C^{1/2})$$

where A' and B' are constants. Straight lines were obtained on plotting $(\eta_{sp}/C)^{-1}$ against $C^{1/2}$ (Fig. 33). Addition of an electrolyte suppresses the loss of mobile ions, hence the rise in η_{sp}/C at low concentrations, was eliminated and the conformity with Huggins equation was restored.

The relative viscosity data at different concentrations were used for the calculation of voluminosity (V_E) of polymer solutions at a given temperature[322,323]. V_E was obtained by plotting Y_1 against concentration C (gm l^{-1}) where

$$Y_1 = (\eta_r^{0.5} - 1) / C (1.35 \eta_r^{0.5} - 0.1)$$

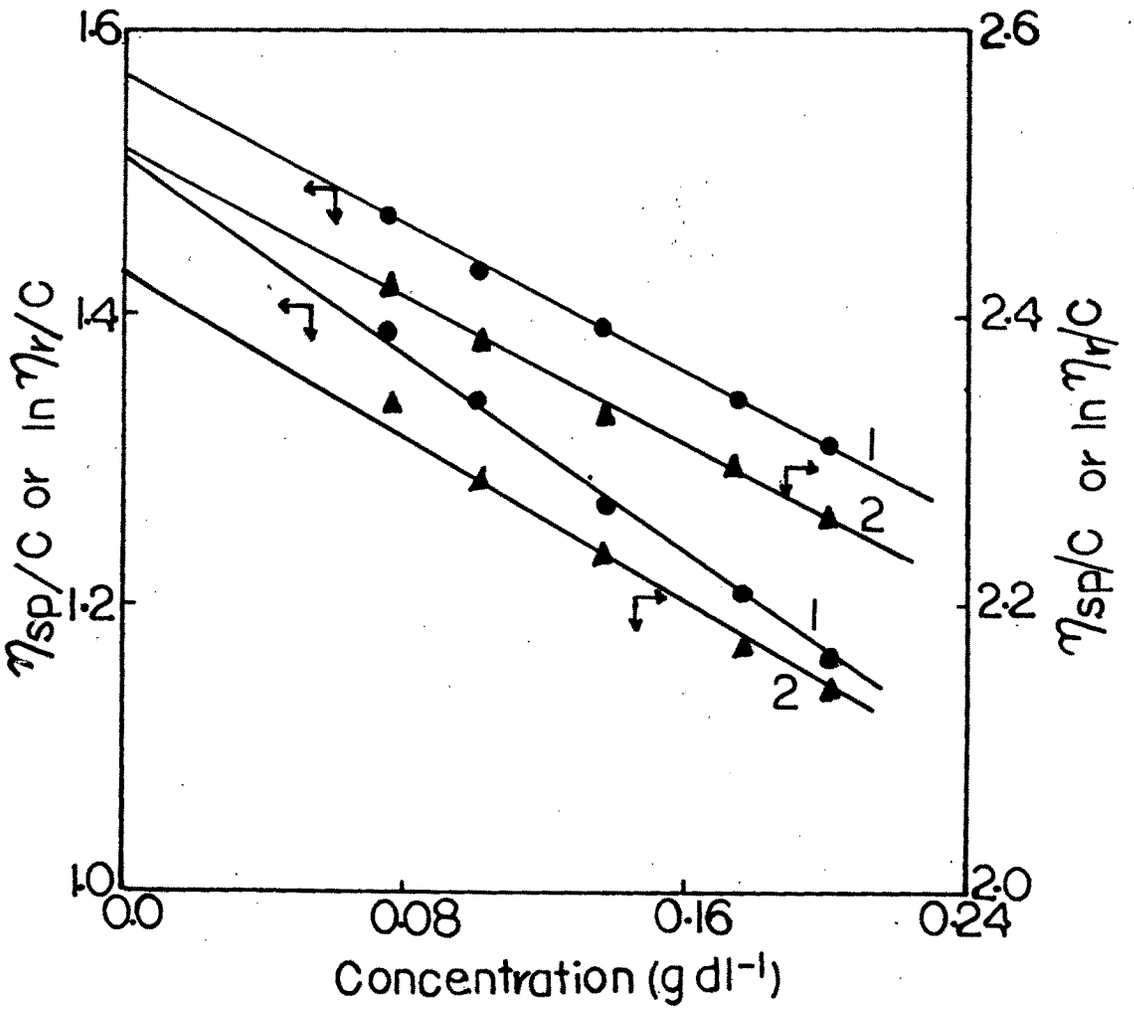

Fig. 32 : Plot of (1) η_{sp}/C; (2) ln η_r/C vs. concentration (g dl^{-1}) for ● P(AA-AAc) 50:50 / 0.5M $NaNO_3$ system at 45°C; ▲ P(AA-AAc) 50:50 / H_2O system at 35°C.

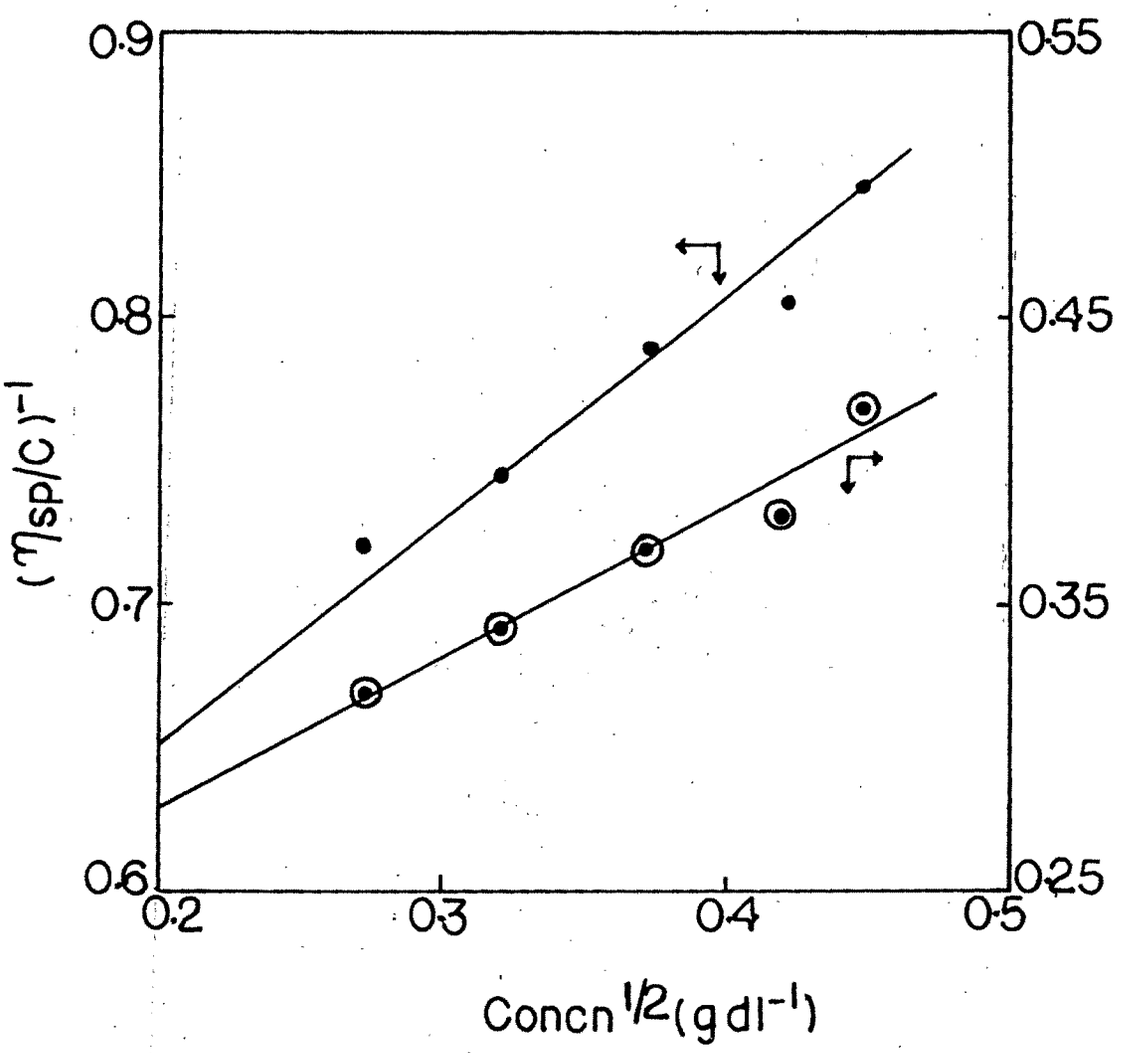

Fig. 33 : Plot of $(\eta_{sp}/C)^{-1}$ vs. (concentration)$^{1/2}$ for the ⊙ P(AA-AAc) 50:50 / H_2O at 35°C; ● P(AA-AAc) / 0.5M $NaNO_3$ at 40°C.

The straight line then obtained was extrapolated to C=O and the intercept yielded V_E. Representative plots are shown in Fig. 34. The values of V_E are listed in Table 6. The shape factor ν was calculated from the equation

$$[\eta] = \nu . V_E$$

The shape factor gives an idea about the shape of macromolecules in solution[331]. It has been used to determine shape of protein molecules in solution[332]. Values of shape factor obtained for various systems are listed in Table 7. All values were ~ 2.5, suggesting spherical conformations for the macromolecules in solution, both in presence and absence of electrolytes. Moreover, ν values were found to be independent of temperature (varying between 2.5 and 2.6) indicating that the minor axis varies by ~ 1%. Various activation parameters of the viscous flow were evaluated using the Frenkel-Eyring equation[333]

$$\eta = Nh/V \exp \Delta G^{\neq}_{vis} / RT$$

where V is the molar volume of the solvent, N is Avogadro number, h is the Plancks constant, R is the gas constant, T is the temperature and $\Delta G^{\neq}_{vis}$ is the free energy of activation for the viscous flow. The above equation can be rewritten as

$$\ln \eta V / Nh = \Delta G^{\neq}_{vis} / RT = \Delta H^{\neq}_{vis} / RT - \Delta S^{\neq}_{vis} / R$$

where $\Delta H^{\neq}_{vis}$ and $\Delta S^{\neq}_{vis}$ are the enthalpy and entropy of activation for the viscous flow[322,324]. $\eta V/Nh$ is an unit less quantity. If η is in centipoise, V is in cm^3/mole, N is molecule / mol and h is J $molecule^{-1}$ then

$$\eta V / Nh = \frac{10^{-1} \times 10^{-4}\ Kg\ m^{-1}\ s^{-1} \times 10^{-6}\ m^3\ mol^{-1}}{molecule \times mol^{-1} \times 10^{-2}\ kg\ m^2\ s^{-1} \times molecule^{-1}}$$

ln ηV / Nh when plotted against T^{-1} (Fig. 35) yields a linear graph with slope and intercept giving $\Delta H^{\neq}_{vis}$ and $\Delta S^{\neq}_{vis}$ respectively. On plotting $\Delta H^{\neq}_{vis}$ and $\Delta S^{\neq}_{vis}$ against concentration of polymer and extrapolating to C=O, $\Delta H^{\neq}_{vis}$ and $\Delta S^{\neq}_{vis}$ values are

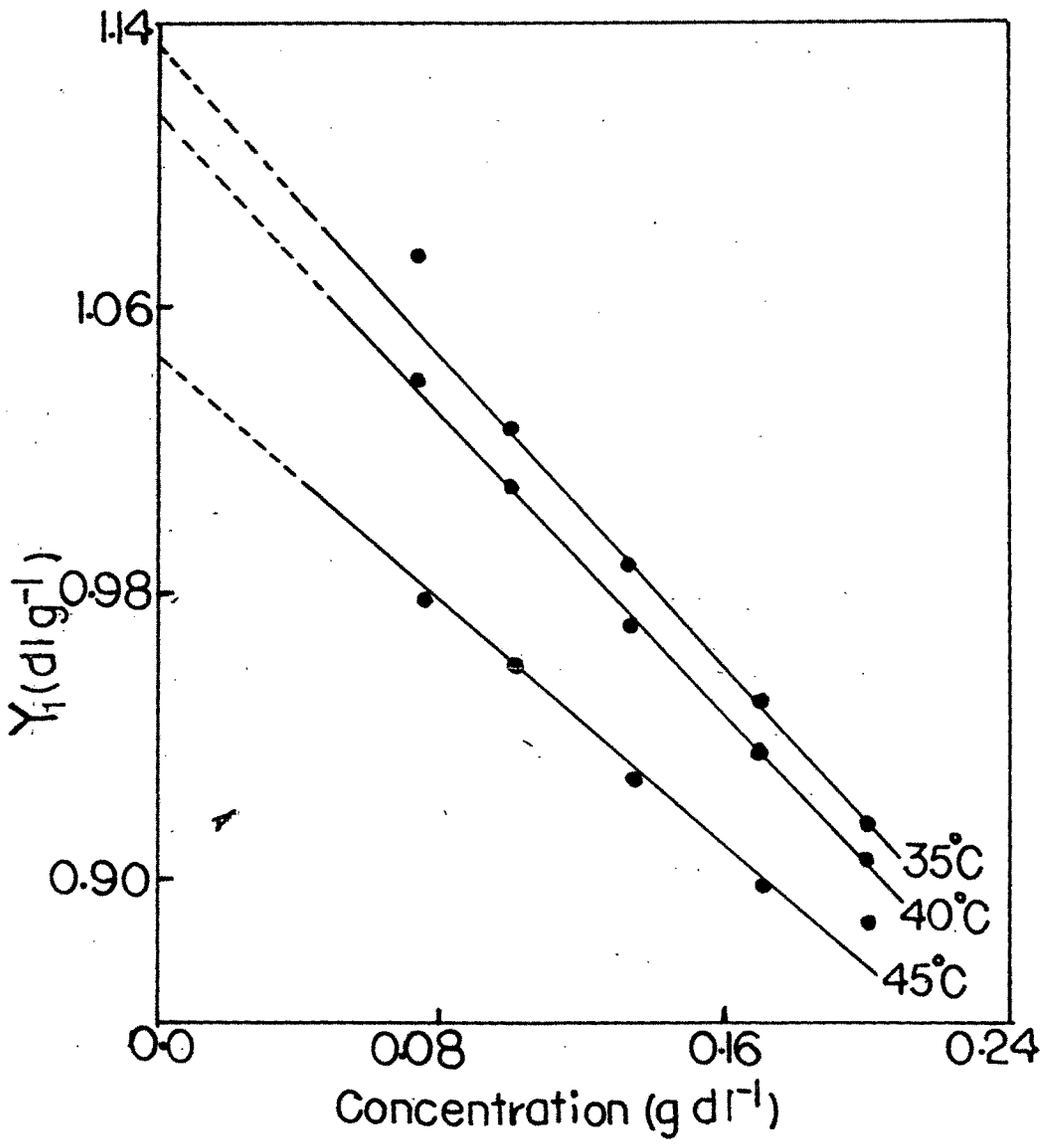

Fig. 34 : Representative plots of Y_1 vs. concentration (g dl^{-1}) for PAA / H_2O system at different temperatures.

Table 6 : Voluminosity of various polymers at different temperatures.

Polymer Systems / Solvent	Voluminosity (V_E)		
	35°C	40°C	45°C
PAA/H_2O	1.16	1.17	1.04
PA/0.05M $NaNO_3$	1.48	1.45	1.34
PAA/0.3M $NaNO_3$	1.49	1.44	1.41
PAA/0.5M $NaNO_3$	1.46	1.48	1.53
PAA/0.1M Al $(NO_3)_3$	1.50	1.45	1.40
PAA/0.3M Al $(NO_3)_3$	1.51	1.54	1.55
PAA/0.5M Al $(NO_3)_3$	1.59	1.60	1.64
P(AA-AAc) 85:15/H_2O	3.10	3.30	3.54
P(AA-AAc) 85:15/0.3M $NaNO_3$	1.01	1.06	1.14
P(AA-AAc) 85:15/0.5M $NaNO_3$	0.90	1.09	1.12
P(AA-AAc) 65:35/H_2O	3.94	3.25	3.58
P(AA-AAc) 65:35/0.05M $NaNO_3$	0.57	0.61	0.64
P(AA-AAc) 65:35/0.1M $NaNO_3$	0.59	0.60	0.65
P(AA-AAc) 65:35/0.5M $NaNO_3$	0.58	0.59	0.63
P(AA-AAc) 50:50/H_2O	2.17	2.53	2.91
PAAc/H_2O	4.19	4.54	4.92

Table 7 : Shape factor (ν) at various temperatures.

Polymer Systems / Solvent	Shape Factor (ν)		
	35°C	40°C	45°C
PAA/H_2O	2.6	2.5	2.5
PA/0.05M $NaNO_3$	2.6	2.6	2.5
PAA/0.3M $NaNO_3$	2.6	2.6	2.5
PAA/0.5M $NaNO_3$	2.6	2.6	2.5
PAA/0.1M Al $(NO_3)_3$	2.6	2.5	2.5
PAA/0.3M Al $(NO_3)_3$	2.6	2.5	2.5
PAA/0.5M Al $(NO_3)_3$	2.6	2.6	2.5
P(AA-AAc) 85:15/H_2O	8.7	10.1	11.7
P(AA-AAc) 85:15/0.3M $NaNO_3$	2.6	2.6	2.6
P(AA-AAc) 85:15/0.5M $NaNO_3$	2.5	2.5	2.6
P(AA-AAc) 65:35/H_2O	8.9	9.8	11.6
P(AA-AAc) 65:35/0.05M $NaNO_3$	2.6	2.6	2.6
P(AA-AAc) 65:35/0.1M $NaNO_3$	2.5	2.6	2.5
P(AA-AAc) 65:35/0.5M $NaNO_3$	2.6	2.6	2.5
P(AA-AAc) 50:50/H_2O	3.4	3.6	3.9
PAAc/H_2O	5.7	6.3	6.9

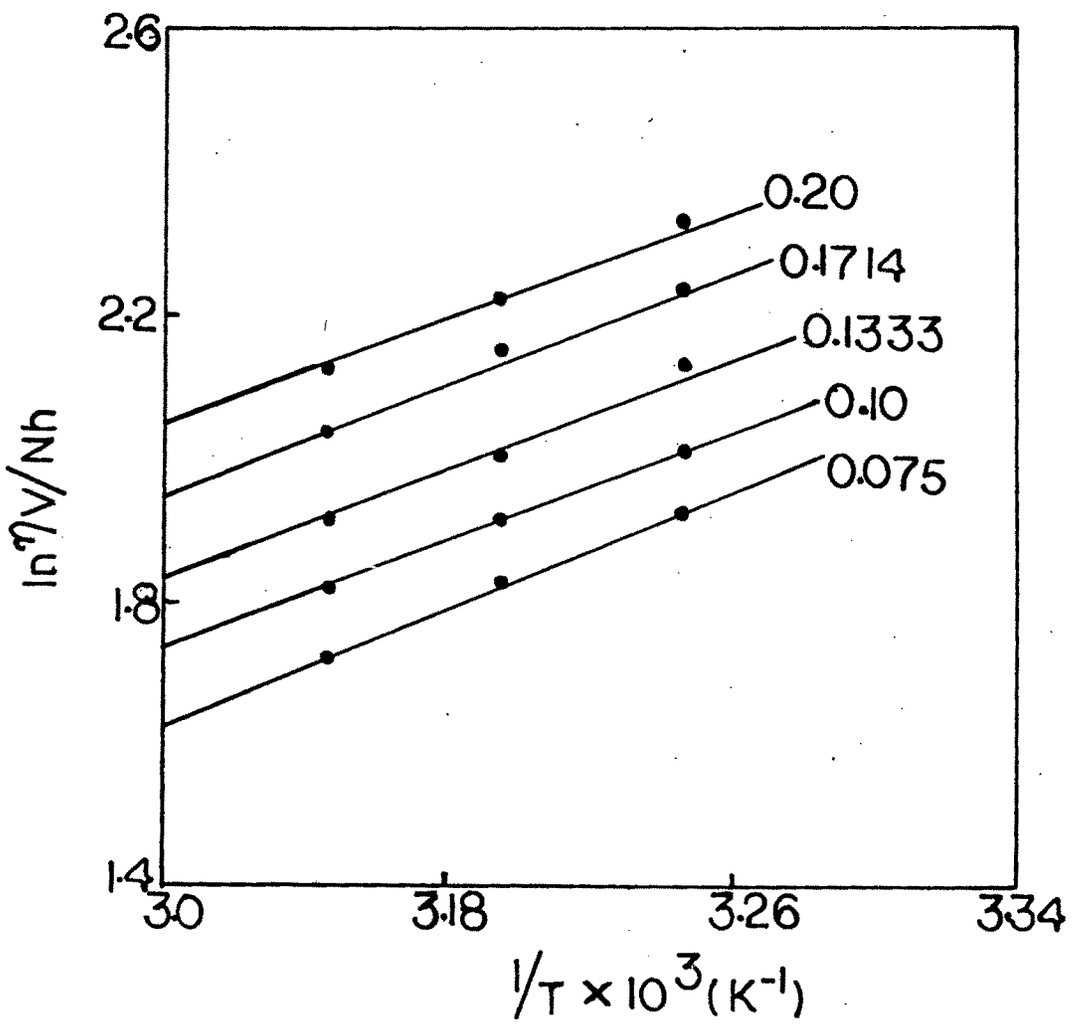

Fig. 35 : Representative plots of ln ηV/Nh vs. 1/T x 10^3 (K^{-1}) for PAA / 0.3 M $NaNO_3$ system.

obtained respectively. $\Delta G^{\neq 0}_{vis}$ values were then computed by the well known thermodynamic relation

$$\Delta G^{\neq 0}_{vis} = \Delta H^{\neq 0}_{vis} - T\,\Delta S^{\neq 0}_{vis}$$

All activation parameters obtained at infinite dilution are given in Table 8. Positive values for $\Delta G^{\neq 0}_{vis}$, $\Delta H^{\neq 0}_{vis}$ and $\Delta S^{\neq 0}_{vis}$ were obtained for all systems studied. The $\Delta H^{\neq 0}_{vis}$ and $\Delta S^{\neq 0}_{vis}$ values vary with electrolyte and also with electrolyte concentration, but no regularity in variations were noted. Interestingly on plotting $\Delta H^{\neq}_{vis}$ versus $\Delta S^{\neq}_{vis}$ for all systems, a linear plot was obtained (Fig. 36). The slope of the plot yielded a temperature of 312 K. Thus at a temperature of 312 K, free energy of activation for the viscous flow becomes independent of entropic forces and is solely governed by the enthalpic forces.

Conclusions :

The characterization of homopolymers polyacrylamide, polyacrylic acid and their copolymers in different monomer feed ratios were carried out by spectroscopic, thermal and viscosity studies.

The IR spectra of the polymers indicate the presence of constituent monomeric units. The copolymers showed characteristic absorption bands of both the monomers. Further evidence of incorporation of two monomers in the copolymers was evidenced by both ^{1}H-NMR spectra and ^{13}C-NMR. The NMR spectra of two hompolymers showed presence of their characteristic groups. In case of the copolymers an extra peak due to methine carbon (-CHCOOH) was observed. The intensity of the peak increased with increase in the amount of AAc incorporated.

The reactivity ratios for the copolymers were determined by both Kelen-Tudos and Finemann-Ross methods. The r_1 and r_2 values obtained by both the methods are 0.427 and 0.945; 0.463 and 1.092 respectively. The structural data like mole fraction composition, blockiness, alternating tendency, mean sequence length of the

Table 8 : Viscosity activation parameters at infinite dilution.

Polymer Systems / Solvent	$\Delta H^{\neq 0}_{vis}$ (k J mol^{-1})	$\Delta S^{\neq 0}_{vis}$ ($Jmol^{-1}$ K^{-1})	$\Delta G^{\neq 0}_{vis}$ (k $Jmol^{-1}$) at 303k
PAA/H_2O	15.9	38	4.5
PA/0.05M $NaNO_3$	12.0	25	4.4
PAA/0.3M $NaNO_3$	16.8	40	4.5
PAA/0.5M $NaNO_3$	15.3	35	4.5
PAA/0.1M Al $(NO_3)_3$	22.5	58	5.0
PAA/0.3M Al $(NO_3)_3$	14.7	31	5.3
PAA/0.5M Al $(NO_3)_3$	14.8	35	4.3
P(AA-AAc) 85:15/H_2O	16.8	40	4.5
P(AA-AAc) 85:15/0.3M $NaNO_3$	16.2	39	4.4
P(AA-AAc) 85:15/0.5M $NaNO_3$	15.3	36	4.4
P(AA-AAc) 65:35/H_2O	16.8	40	4.5
P(AA-AAc) 65:35/0.05M $NaNO_3$	11.2	22	4.5
P(AA-AAc) 65:35/0.1M $NaNO_3$	21.4	55	4.7
P(AA-AAc) 65:35/0.5M $NaNO_3$	8.8	15	4.3
P(AA-AAc) 50:50/H_2O	12.3	25	4.6
PAAc/H_2O	19.8	50	4.4

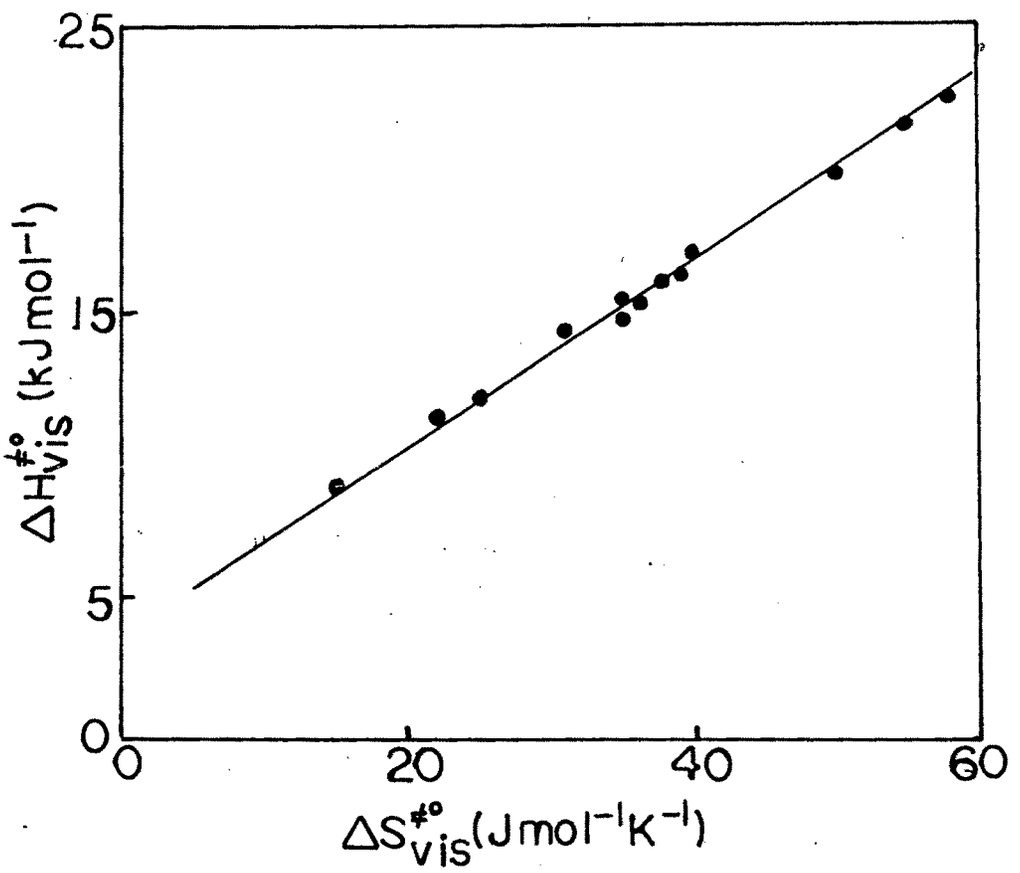

Fig. 36 : Enthalpy-entropy compensation plot for all the polymer systems.

copolymers were evaluated from the reactivity ratios data. It can be concluded that the copolymers are random rather than alternating.

Thermal characterization of the polymers was done by TGA and DSC techniques. The thermograms of the copolymers fall in between that of the homopolymers indicating copolymers have intermediate thermal stability. The activation energy (E) values were evaluated using different empirical equations. The copolymers and PAAc showed two staged decompositions - whereas PAA showed three staged decompositions.

The viscosity studies of the polymers showed, that copolymers behaved like polyelectrolytes. They had large [η] values in water. On addition of an electrolyte the conformity with Huggins and Kraemer equation was restored. The shape factor values were evaluated from relative viscosity data. The shape factor 'ν' values were found to be ~ 2.5 both in presence and absence of electrolytes, indicating spherical conformation in solution. From the viscosity data, activation parameters for the viscous flow were evaluated. An enthalpy - entropy compensation was observed for these systems.